1969

Behavior of granular materials under triaxial compression with pulsating deviator stress

Jerry James Marley
Iowa State University

69-15,628

MARLEY, Jerry James, 1935-

BEHAVIOR OF GRANULAR MATERIALS UNDER TRIAXIAL COMPRESSION WITH PULSATING DEVIATOR STRESS.

Iowa State University, Ph.D., 1969
Engineering, civil

University Microfilms, Inc., Ann Arbor, Michigan

BEHAVIOR OF GRANULAR MATERIALS UNDER TRIAXIAL COMPRESSION WITH PULSATING DEVIATOR STRESS

by

Jerry James Marley

A Dissertation Submitted to the
Graduate Faculty in Partial Fulfillment of
The Requirements for the Degree of
DOCTOR OF PHILOSOPHY

Major Subject: Civil Engineering

Approved:

Signature was redacted for privacy.
In Charge of Major Work

Signature was redacted for privacy.
Head of Major Department

Signature was redacted for privacy.
Dean of Graduate College

Iowa State University
Ames, Iowa

1969

TABLE OF CONTENTS

INTRODUCTION

The solution of engineering problems which involve soils or aggregates requires knowledge of the material properties, the nature of the imposed stresses and other contemplated environmental changes, and the response of the material to the environmental changes. Among these requirements, the most easily determined is the environmental changes. A considerable body of knowledge also exists pertaining to the material properties and response due to certain types of stresses and modes of stress applications.

One very common mode of stress application about which relatively little is known concerning the response of the material is the repeated application and removal of compressive and flexural stresses on highway or airfield pavements.

As a result of the lack of knowledge to adequately describe the response of materials to repeatedly applied stresses, the solutions of pavement design problems have rested largely on empirical knowledge gained from observations on in-service and full scale test pavements. Because of the inability to control all environmental variables under such conditions, the results of such observations have been largely qualitative.

The objective of this study was to determine the nature of the response of a crushed limestone aggregate subjected to repeatedly applied compressive stresses in the controlled environment of the laboratory, and thus determine those material properties which are pertinent to the behavior of materials subjected to this mode of stress application.

This study was carried out using a triaxial compression apparatus on compacted specimens of crushed limestone, either untreated or treated with

asphalt cement as a stabilizing additive. The triaxial apparatus was designed to apply repeated uniaxial stress under controlled temperature conditions.

REVIEW OF LITERATURE

Studies of the shearing resistance of soils often begin with an assumption that behavior of the material is described by the Coulomb equation:

$$\tau = C + P_n \tan \phi \qquad (1)$$

where

τ is shear stress,

C is cohesion,

P_n is the stress normal to the shear stress, and

ϕ is the angle of internal friction.

There are, however, certain difficulties with this approach. Values of the parameters C and ϕ may not only be a function of the material but also of the type and conditions of the test by which they are determined. Because of the dependence of the value of these parameters on test conditions, any determination of the parameters under test conditions other than those corresponding to prototype conditions is of limited value.

The Mohr-Coulomb theory describes the behavior of the material at a failure condition where total rupture of the soil mass takes place. The Coulomb equation and the Mohr-Coulomb theory provide no information on the deformation resulting from the application of stresses lower than the failure stresses, or on any cumulative effects due to repeatedly applied sub-failure stresses.

Since the problem of pavement design involves the determination of a pavement structure which will sustain the repeated application of many thousands of wheel loads with neither total rupture nor excessive deformation of the pavement structure, the Mohr-Coulomb theory is inadequate to

describe the behavior of materials under such stress conditions.

The Coulomb parameters, C and Ø as determined by conve ional, controlled strain triaxial testing have been qualitatively correlated to performance of in-service and full scale test pavements with limited success.

Repeated load triaxial testing is a relatively recent approach in the soil and highway engineering field and, while interesting aspects of the behavior of materials subjected to this type of loading have been reported by Havers and Yoder (1957), Haynes and Yoder (1963), Seed and Chan (1957, 1958), Seed et al. (1955), Seed et al. (1958), and Seed and McNeill (1956, 1957), little attempt has been made by any of these authors to describe observations other than phenomenologically, probably due to the fact that there is no generally accepted behavioral model available by which the observations could be related.

It was observed by Larew and Leonards (1962) that the behavior of soil materials subjected to repeated loads appeared to be analogous to the behavior of soil materials subjected to creep loading, that is, a time-dependent deformation under constant stress. This seems reasonable, considering the fact that the number of applications of a repeatedly applied stress is a function of the frequency of load applications multiplied by elapsed time:

$$N = f \times t \tag{2}$$

where

N is the number of load applications,

f is the frequency of load applications, and

t is the elapsed time.

From this very simple relationship it is possible to envision that, since the number of load applications is a function of time, the behavior of material subjected to a constant stress for some period of time, and the behavior of material subjected to a constant stress intermittently applied a number of times, may well be analogous.

Recently, the theory of rate processes has been applied to the time-dependent behavior of soils and highway pavement materials by Herrin and Jones (1963), Herrin et al. (1966), Christensen and Wu (1964), Mitchell (1964), Mitchell and Campanella (1964), Mitchell et al. (1968), Moavenzadeh and Stander (1966), Noble (1968), Secor and Monismith (1965) and Pagen (1965) with a considerable degree of success.

The potential for the application of the theory of rate processes to processes as widely divergent as chemical reactions and the shear deformation of particulate systems such as soil or mineral aggregates was recognized by the authors of one of the early definitive works on the theory of rate processes when they wrote: (Glasstone et al., 1941, p. vii)

> ...the theory of absolute reaction rates is not merely a theory of the kinetics of chemical reactions; it is one that can, in principle, be applied to any process involving a rearrangement of matter, that is to say, any 'rate process'.

The application of the theory of rate processes to the creep behavior of metals has been known for some time and has been investigated by Dorn (1957), Ree et al. (1963), Andrade (1951, 1957), and Schoeck (1957). Considerable data has been accumulated which has allowed many authors to hypothesize deformation mechanisms which agree with observed kinetic data.

Attention has also been given to the application of rate process theory to the deformation of ice and snow by Barnes and Tabor (1966), Glen (1955), Glen (1953), Landauer (1955), Kingery (1960), Telford and Turner (1963) and Gold (1967). Hahn et al. (1967) applied the theory to the plastic deformation of marble, Goughnour and Andersland (1968) to a sand-ice system and Ree and Eyring (1955) and Andrade (1951) to generalized plastic solid systems.

In addition, the applicability of the rate process theory to the shearing deformation or viscosity of fluids has been known for some time, and this particular application has been treated by Glasstone et al. (1941) in some detail.

The applicability of the theory of rate processes to the behavior of metals subjected to intermittently applied stresses has been investigated by Caughey and Hoyt (1954), Smith and Houston (1954), Simmons and Cross (1954), Manson and Brown (1959), and Feltner and Sinclair (1963). These investigators found the rate process theory to adequately describe the observed behavior, although there is no general agreement among them on the relationship between "static" and "cyclic" creep. The relationship between the amount and rate of deformation as observed by these investigators for materials subjected to constant stress and intermittent stress, is apparently dependent on the various stress levels used, temperature conditions, and other test variables utilized by the individual investigators.

THEORY

If a material does not instantaneously deform under load, deformation of its mass requires an input of energy. In the particulate systems considered in this study, this energy is required to: (1) break or deform any bonds (friction or cohesion) which exist between particles or groups of particles; and (2) to change or rearrange the relative configuration of one particle or group of particles relative to another particle or group, if this rearrangement requires a change in the volume of the material. This energy is released by the material system when the interparticle bonds reform and particles and groups return to their initial configuration.

The rate at which deformation takes place is a function of strength of interparticle bonds, relative configuration of the particles or groups and the rate of energy input into the system.

Chemical kinetic theory provides a means by which the deformation rate, and those material properties which affect the rate of deformation, can be related. The theory of rate processes cannot provide information on the state of the material prior to, during, or at the completion of a reaction or rearrangement of material, but can provide information on the rate at which the reaction or rearrangement takes place. The state of the material prior to, or at any time during, the reaction process has an effect on the rate and any such effect must be experimentally determined in order to develop an equation which will adequately describe the rate process involved.

In any system of matter there are continuous movements. These movements are, in the absence of any external stress, non-directional or, more

precisely, are randomly directed and result in no net movement of the material. The application of an external stress to such a system results in a net movement in the direction of the imposed stress. This concept has been stated by Eyring (1967, p. 20):

> Electrical potentials, or other kinds of stress, applied to any system do not ordinarily initiate a new process but simply bias existing rates, thereby modifying the rate of passing to equilibrium.

The application of a stress alters the rate of, and gives direction to, an already existing process; it is this directional "biased" rate of passing to equilibrium that is the concern of this study.

In chemical kinetics, the rate constant of chemical reactions is represented by the Arrhenius equation (Moore, 1962),

$$k = A \exp \frac{-E_a}{RT} \qquad (3)$$

where

k is the specific rate constant,

A is a pre-exponential multiplier, often referred to as the Arrhenius frequency factor,

E_a is the activation energy of the process,

R is the universal gas constant, and

T is the absolute temperature at which the reaction occurs.

Equation 3 is now generally accepted as an adequate representation of the temperature dependence of any rate process, as Glasstone et al. (1941, p. 1) stated:

> ...it is now generally accepted that a relationship of this kind represents the temperature dependence of the specific rates of most chemical reactions, and even of certain physical processes....

Energy concepts

For purposes of this study, it is assumed that the resistance of a soil to shear deformation results from the existence of an energy barrier for bonding units in the material. This energy barrier results from two factors as mentioned previously; viz. bonds between particles or groups, and other resistance to rearrangement of particles or groups of particles. This energy barrier is the so called activation energy. The number of bonding units which have energy great enough to surmount the energy barrier, that is the number of bonding units with energies greater than the activation energy of the material, is given by the Maxwell-Boltzman distribution law. The rate of bonding units passing over the energy barrier is proportional to the number of bonding units with energy greater than, or equal to, the activation energy.

The number of bonding units which pass over the energy barrier per unit time is then a measure of the rate of deformation of the material and may be expressed as

$$\dot{\epsilon} = K \exp - \frac{\Delta F^*}{kT} \tag{4}$$

where

$\dot{\epsilon}$ is the rate of deformation,

K is a proportionality constant,

ΔF^* is the activation free energy of the material,

k is the Boltzman constant, and

T is the absolute temperature at which the deformation occurs.

The energy barrier with no externally applied stresses is illustrated

in Figure 1 by the solid line.

The applied stresses in a triaxial compression test are illustrated in Figure 2, σ_1 being the major principal stress and σ_3 the minor principal stress. Considering the stresses acting on an element of the material such as element A, shown in Figure 2a, and expanded in Figure 2b, the imposed stresses are resolved into normal and tangential stress components, designated P_n and τ respectively.

The work done in deforming this element of soil from configuration 1 shown with solid lines in Figure 2b to a configuration such as 2 (shown by dashed lines), consists of breaking interparticle bonds and changing the volume of the element against the normal stress P_n. The work done in breaking one interparticle bond is the stress on the bond multiplied by the volume of the bonding unit. The stress on the bond is τ and designating the volume of a bonding unit as β', the energy required to break one interparticle bond is $-\beta'\tau$, the energy acquired by the bonding unit in going over the energy barrier. The work required to change the volume of material from configuration 1 to 2 is $P_n(V_2-V_1)$ or $P_n \Delta V$, representing the total volume change work done on this element. The volume change work done on the element per unit volume of bonds is the volume change work done on the element multiplied by the ratio of the volume of a bonding unit to the total volume of the element or $\frac{\beta'}{V} P_n \Delta V$. The total work required to deform the element is then $-\beta'\tau + \frac{\beta'}{V} P_n \Delta V$ or $\beta'(-\tau + P_n \frac{\Delta V}{V})$.

The height of the energy barrier designated as ΔF^* in Figure 1 therefore is changed by an amount $\beta'(-\tau + P_n \frac{\Delta V}{V})$ when an external stress is

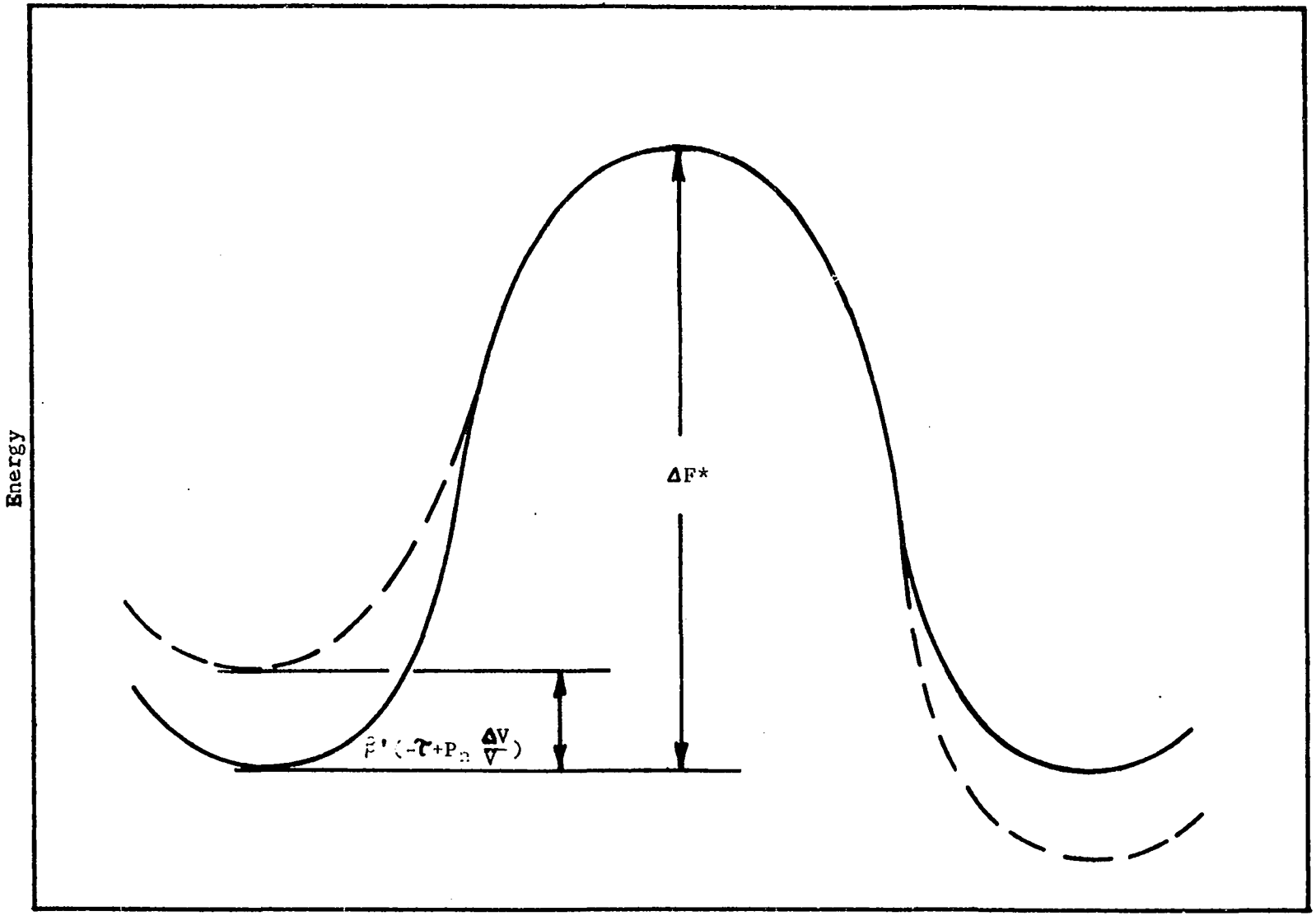

Figure 1. Energy barrier for deformation, with and without shear stress

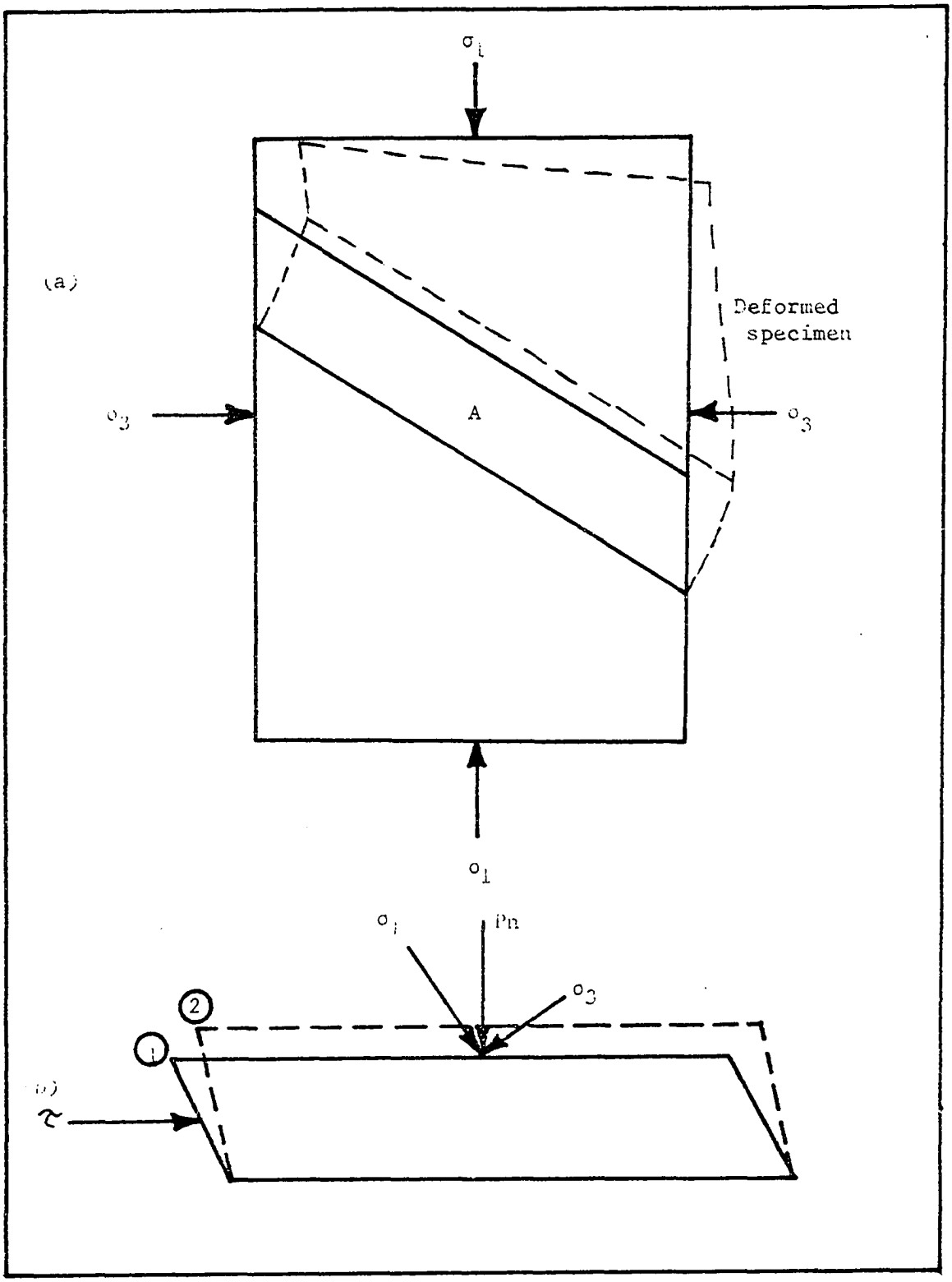

Figure 2. Applied stresses in triaxial shear testing

applied to the system as shown by the dashed lines in Figure 1. The effect of the term $P_n \frac{\Delta V}{V}$ depends on the nature of the change in the volume of the material. If the volume must be increased, $\beta' P_n \frac{\Delta V}{V}$ represents energy which must be surmounted by the bonding unit, and the activation energy is increased by this amount. If volume is decreased by deformation, $\beta' P_n \frac{\Delta V}{V}$ represents energy acquired by the bonding unit and activation energy is decreased by this amount. Since an increase in volume was considered in this derivation, the effects of shear stress and volume change on activation energy are of opposite sign.

Introducing the relationship from thermodynamics that

$$\Delta F^* = \Delta H^* - T\Delta S^* \tag{5}$$

where

ΔH^* is the activation enthalpy,

ΔS^* is the activation entropy, and

other terms are as previously defined,

and considering the further subdivision of ΔF^* when an external shear stress is applied as developed above,

$$\Delta F^* = \Delta H^* - T\Delta S^* - \beta'\tau + \beta' P_n \frac{\Delta V}{V} . \tag{6}$$

Substituting equation 6 into equation 4,

$$\dot{\epsilon} = K \exp -\frac{\Delta H^*}{kT} \exp \frac{\Delta S^*}{k} \exp \frac{\beta'\tau}{kT} \exp - \frac{\beta'}{kT} P_n \frac{\Delta V}{V} . \tag{7}$$

If it is now assumed that ΔS^* is independent of temperature, this term may be included in the pre-exponential coefficient, and further, setting $\beta = \frac{\beta'}{kT}$, equation 7 becomes

$$\dot{\epsilon} = K' \exp -\frac{\Delta H^*}{kT} \exp \beta\tau \exp - \beta P_n \frac{\Delta V}{V} . \tag{8}$$

Soil structure

The relationship expressed by equation 8 indicates that the rate of deformation is independent of total deformation (other than that represented by volume change) and time, since neither of these quantities appear on the right side. It has been tacitly assumed, however, in the derivation of equation 8 that any change in the structure of the material is completely represented by the change in the volume of the material. Also, time-dependence of deformation rate is implicit in equation 8 since volume change is time dependent.

Time dependence of the rate of deformation represents a problem in the general applicability of equation 8 to the shear deformation of soils, since in order to be useful in determining the effect of varying τ on the deformation rate, the deformation rate at constant τ must be constant, or the functional relationship between time and deformation rate must be known.

Since the constancy of the rate of deformation can be assured by determining the rate of deformation at the point where the derivative of the deformation rate is zero, i.e. $\ddot{\epsilon} = 0$, this seems to be a much simpler criterion for determining a meaningful deformation rate than attempting to determine a functional relationship between deformation rate and time. However, since none of the terms on the right side of equation 8 can be zero and the derivative of $\exp -\beta P_n \frac{\Delta V}{V}$ is, in general, not zero, this equation is inadequate to represent the deformation rate of soils unless some further relationships are known.

Since there is experimental evidence that the rate of deformation is a function of deformation (or time), this relationship should be included

in equation 8 so that

$$\dot{\epsilon} = K' \exp \frac{-\Delta H^*}{kT} \exp \beta \tau \exp - \beta P_n \frac{\Delta V}{V} \cdot f(\epsilon) \qquad (9)$$

where $f(\epsilon)$ is an unknown function of the deformation.

Both $f(\epsilon)$ and $\frac{\Delta V}{V}$ are measures of the rearrangement of the material during deformation, or combined, represent a change in the structure of the material during deformation. Representing these combined effects by a single factor S, which is an unknown function describing the dependence of the rate of deformation on any changes in the structure of the material during deformation, equation 9 becomes

$$\dot{\epsilon} = K' \exp - \frac{\Delta H^*}{kT} \exp \beta \tau \cdot S \cdot \qquad (10)$$

Equation 10 expresses a relationship between deformation rate, activation enthalpy, shear stress and structure, but the structure factor S is an unknown function and this equation is of little value unless the effect of this function of structure can be determined or eliminated. Since the structure function is probably a complex function, the possibility of eliminating the effects of this function will be considered.

One obvious possibility is to consider the relationships of strain rate and other variables at a condition of constant structure in each specimen tested. Under these conditions, the effect of structure would be constant and could be included in the pre-exponential coefficient.

With the introduction of the criterion of constant structure, equation 10 is a useful relationship provided that two conditions are met when the equation is applied: (1) that $\ddot{\epsilon} = 0$ and (2) that a constant structure exists. But a means of insuring constant structure is necessary.

It is assumed that the initial structure of material specimens prepared in the same manner is essentially constant (or more realistically, is normally distributed about some mean value of the structure parameter) and, that it is possible for each specimen, as it is deformed under differing test conditions, to attain another value of the structure parameter which is identical in all specimens. The structure at any time after the start of a test is a function of time, shear stress, temperature and normal stress or

$$S = f(\tau, P_n, T, t). \tag{11}$$

There are other functional relationships of structure that could be considered. For instance, t could be replaced by deformation, ϵ, but the variables chosen are obvious, independent variables that are assumed for the development of the theory.

Differentiating equation 11 at constant temperature and normal stress,

$$dS = \left(\frac{\partial S}{\partial \tau}\right)_{T,P_n,t} d\tau + \left(\frac{\partial S}{\partial t}\right)_{T,P_n,\tau} dt \quad . \tag{12}$$

Introducing the condition that when the structure function is constant, $dS = 0$, and setting the right side of equation 12 equal to zero,

$$\left(\frac{\partial S}{\partial \tau}\right)_{T,P_n,t}\left(\frac{\partial \tau}{\partial t}\right)_{T,P_n,S} + \left(\frac{\partial S}{\partial t}\right)_{T,P_n,\tau} = 0 \quad . \tag{13}$$

Again differentiating equation 11 but at constant temperature and shear stress,

$$dS = \left(\frac{\partial S}{\partial P_n}\right)_{T,\tau,t} dP_n + \left(\frac{\partial S}{\partial t}\right)_{T,\tau,P_n} dt \tag{14}$$

and setting the right side of this equation equal to zero,

$$\left(\frac{\partial S}{\partial P_n}\right)_{T,\tau,t}\left(\frac{\partial P_n}{\partial t}\right)_{T,\tau,S} + \left(\frac{\partial S}{\partial t}\right)_{T,\tau,P_n} = 0 \; . \qquad (15)$$

Differentiating equation 10 with respect to time at constant temperature, shear stress and normal stress,

$$\ddot{\epsilon} = K' \exp - \frac{\Delta H^*}{kT} \exp \beta\tau\left(\frac{\partial S}{\partial t}\right)_{T,\tau,P_n} \; . \qquad (16)$$

At the point where $\ddot{\epsilon} = 0$, the right side of equation 16 must be zero. Since the only term on the right side of this equation which can be zero is $\left(\frac{\partial S}{\partial t}\right)_{T,\tau,P_n}$, this term must be zero when $\ddot{\epsilon} = 0$. Thus, when one necessary condition for the valid application of equation 10 is met, viz. $\ddot{\epsilon} = 0$, $\left(\frac{\partial S}{\partial t}\right)_{T,\tau,P_n}$ is also zero.

Substituting this relationship into equations 13 and 15, when $\ddot{\epsilon} = 0$

$$\left(\frac{\partial S}{\partial \tau}\right)_{T,P_n,t}\left(\frac{\partial \tau}{\partial t}\right)_{t,P_n,S} = 0 \text{ and } \left(\frac{\partial S}{\partial P_n}\right)_{T,\tau,t}\left(\frac{\partial P_n}{\partial t}\right)_{T,\tau,S} = 0$$

if the structure remains constant. These conditions may be satisfied if either the products are zero or if one of the terms in either equation is zero.

In general, neither $\left(\frac{\partial \tau}{\partial t}\right)_{T,P_n,S}$ nor $\left(\frac{\partial P_n}{\partial t}\right)_{T,\tau,S}$ are zero, because if they were, this would indicate that there is no relationship between τ and t or P_n and t, which is contrary to experimental evidence. If the relationship between τ and t, or P_n and t, were such that it had a maximum or minimum value, the partial derivatives would have zero values at that point. However, in order for these relationships to have maximum or minimum values,

there would have to be a value of the structure function at a low value of τ or P_n which is duplicated at a higher value of τ or P_n, whereas at an intermediate value of τ or P_n, the value of the structure function would be either greater or less than that occurring at higher or lower values of τ or P_n. Since it does not seem reasonable to expect that this would occur, it is very unlikely that either $\left(\frac{\partial \tau}{\partial t}\right)_{T,P_n,S}$ or $\left(\frac{\partial P_n}{\partial t}\right)_{T,\tau,S}$ have zero values.

If neither $\left(\frac{\partial \tau}{\partial t}\right)_{T,P_n,S}$ nor $\left(\frac{\partial P_n}{\partial t}\right)_{T,\tau,S}$ have zero values, then $\left(\frac{\partial S}{\partial \tau}\right)_{T,P_n,t}$ and $\left(\frac{\partial S}{\partial P_n}\right)_{T,\tau,t}$ must be zero whenever $\left(\frac{\partial S}{\partial t}\right)_{T,\tau,P_n}$ equals zero, which is at the point of inflection, i.e. when $\ddot{\epsilon} = 0$.

In summary, this argument states that $\left(\frac{\partial S}{\partial t}\right)_{T,\tau,P_n}$ and $\left(\frac{\partial S}{\partial \tau}\right)_{T,P_n,t}$ or $\left(\frac{\partial S}{\partial P_n}\right)_{T,\tau,t}$ are zero at any point of inflection, which means, that at points of inflection, the structure remains constant when t, τ, or P_n is varied.

The relationship for constant structure has been developed for constant temperature. However, the same line of reasoning would lead to the consideration of the possibility of $\left(\frac{\partial T}{\partial t}\right)_{\tau,P_n,S}$ having a zero value and result in conclusions similar to those above.

Failure criteria and deformation

The use of $\ddot{\epsilon} = 0$ as a criterion for applying the rate equation to determine the effect of stress on the rate of deformation is very common in creep testing of metals (Dorn, 1957; Schoeck, 1957), because the deformation rate used by these researchers is the rate in a secondary creep portion of the

time-deformation curve where the deformation rate is constant. Time-deformation relationships are usually considered to consist of several different stages, as illustrated in Figure 3. Stage I is the instantaneous deformation which occurs when the load is applied; Stage II is transient creep in which the deformation rate decreases and may terminate under low stresses as shown in curve a of Figure 3. Stage III represents steady state creep characterized by a constant rate of deformation, and stage IV is "tertiary" creep characterized by accelerating deformation and leads to rupture as shown typically in curve b of Figure 3.

It has been found by some researchers (Noble, 1968; Singh and Mitchell, 1968) that steady state creep seldom occurs for any significant time period in soils tested in direct or triaxial shear. However, in creep tests which exhibit a transient creep zone and a tertiary creep zone, there is a point of inflection in the time-deformation curve at which point the second derivative of deformation with respect to time is zero, even though there may not be evidence of a significant period of steady state creep.

Failure criteria have been proposed by Schmidt (1962b) as the point at which the strain acceleration becomes positive (i.e. the point where $\ddot{\epsilon}$ becomes greater than zero); by Hughes (1967) as the point of inflection on the strain repetition curves for repetitive loading of asphaltic concrete. The Hughes criterion is identical to the $\ddot{\epsilon} = 0$ criterion and, if the material exhibits no secondary creep, the Schmidt criterion is also essentially the same. Noble (1968) also proposed the criterion of $\ddot{\epsilon} = 0$ for determining a meaningful rate of deformation in applying the rate equation to soil deformation.

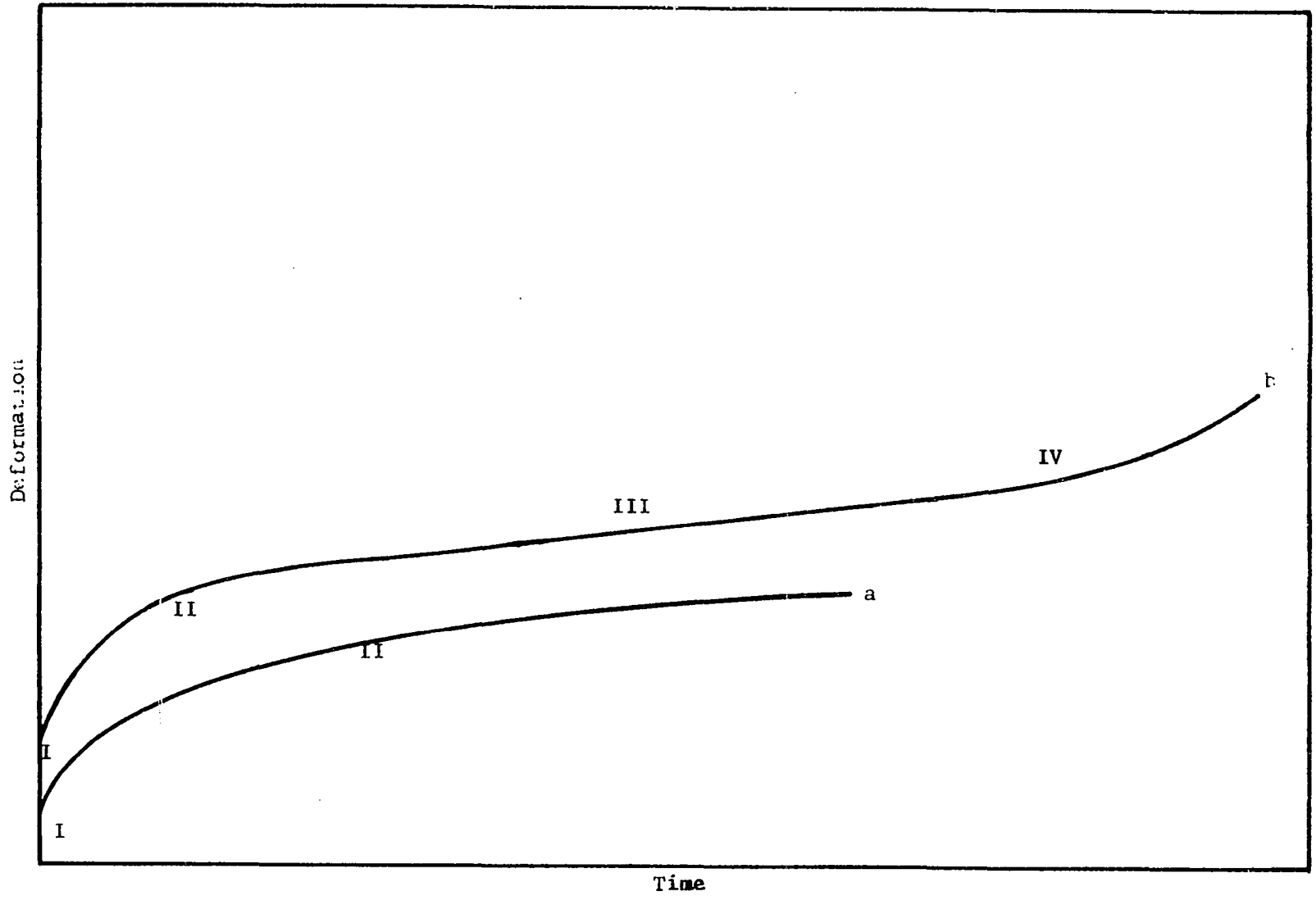

Figure 3. Generalized deformation versus time relationships

The conditions under which the rate equation is applicable to soil deformation, as developed above for constant structure, is consistent with any of the proposed failure criteria. Equation 10 may now be written

$$\dot{\epsilon} = K'' \exp -\frac{\Delta H^*}{kT} \exp \beta\tau \qquad (17)$$

where K'' is a coefficient that includes the proportionality constant, the entropy of activation and the effect of structure.

Equation 17 describes the effects of shear stress and temperature on the rate of deformation at a point which might be defined as incipient rupture. However, in many engineering applications, incipient rupture is not a satisfactory failure criterion, because deformations which are detrimental to the intended use of the engineering structure may occur prior to rupture. One such application is that of highway and airfield pavements where the pavement may exhibit deformations detrimental to its function prior to rupture of the pavement mass.

Therefore, it is very desirable to be able to relate the amount of deformation to shear stress, normal stress and temperature. In order to do this, the functional relationship between deformation and time in the transient creep portion of the time-deformation curve is needed. Considerable work has been done on this aspect of the behavior of metals, and a functional relationship has been proposed by Andrade (1951):

$$\epsilon - \epsilon_o = b\, t^{1/3} \qquad (18)$$

where

ϵ is the total deformation,

ϵ_o is the instantaneous (elastic) deformation which occurs with the application of the stress,

b is a proportionality constant, and

t is the elapsed time after the application of the stress.

Differentiating this equation,

$$\dot{\epsilon} = \frac{b}{3} t^{-2/3} \tag{19}$$

and solving for t from equation 18,

$$t = \frac{(\epsilon - \epsilon_o)^3}{b^3} . \tag{20}$$

Substituting the relationship for t in equation 20 into equation 19,

$$\dot{\epsilon} = \frac{b}{3} \left[\frac{(\epsilon - \epsilon_o)^3}{b^3} \right]^{-2/3} = \frac{b^3}{3} \frac{1}{(\epsilon - \epsilon_o)^2} . \tag{21}$$

If the value of ϵ_o is very small compared to ϵ, its effect can be neglected and

$$\dot{\epsilon} = \frac{b^3}{3} \frac{1}{\epsilon^2} . \tag{22}$$

There are now two equations for the rate of deformation, one derived from theoretical principles and the other an empirically proposed relationship which later will be shown to be consistent with the results of this investigation.

If $\frac{1}{\epsilon^2}$ is the unknown function of deformation in equation 9 and the coefficient b^3 of equation 22 is represented by the other terms on the right side of equation 9, the rate equation becomes

$$\dot{\epsilon} = \frac{K'}{3} \exp - \frac{\Delta H^*}{kT} \exp \beta\tau \exp - \beta P_n \frac{\Delta V}{V} \cdot \frac{1}{\epsilon^2} . \tag{23}$$

In this form, the rate equation is more complex than equation 17 and as such is a less desirable form for evaluating the parameters ΔH^* and β,

but by separating variables and integrating this equation, a relationship between total deformation and other variables results:

$$\epsilon^3 = K' \exp - \frac{\Delta H^*}{kT} \exp \beta\tau \exp - \beta P_n \frac{\Delta V}{V} \cdot t \ . \qquad (24)$$

Because of its empirical nature and the assumptions used in its derivation, the validity of equation 23 can only be ascertained by experimental evidence. The inclusion of several interdependent variables in the equation poses the question as to whether the correct functional relationship among them is stated in equation 23. For example, the effect due to $\frac{\Delta V}{V}$ in equation 9 may be included in $\frac{1}{\epsilon^2}$ in equation 22 rather than in b^3 as was assumed in writing equation 23.

Implications of equation 23 may be further examined to determine if this equation implies conditions which are contrary to any basic laws. One such condition implied by equation 23 is the relationship between total deformation and volume change when $\ddot{\epsilon} = 0$.

The time derivative of equation 23 at constant τ, P_n, and T, since K', T and τ are independent of time, is:

$$\dot{\epsilon} = \frac{K'}{3} \exp - \frac{\Delta H^*}{kT} \exp \beta\tau \frac{d}{dt} \left[\exp - \beta P_n \frac{\Delta V}{V} \cdot \frac{1}{\epsilon^2}\right]$$

$$\ddot{\epsilon} = \frac{K'}{3} \exp - \frac{\Delta H^*}{kT} \exp \beta\tau [-\beta P_n \exp - \beta P_n \frac{\Delta V}{V} \cdot \frac{1}{\epsilon^2} \frac{d\, \Delta V/V}{dt} + \frac{-2}{\epsilon^3} \exp -\beta P_n \frac{\Delta V}{V} \frac{d\epsilon}{dt}]$$

$$\ddot{\epsilon} = \frac{K'}{3} \exp - \frac{\Delta H^*}{kT} \exp \beta\tau \exp - \beta P_n \frac{\Delta V}{V} \cdot \frac{1}{\epsilon^2} [-\beta P_n \frac{d\Delta V/V}{dt} - \frac{2}{\epsilon} \frac{d\epsilon}{dt}] \qquad (25a)$$

or

$$\ddot{\epsilon} = \dot{\epsilon} [-\beta P_n \frac{d\Delta V/V}{dt} - \frac{2}{\epsilon} \frac{d\epsilon}{dt}] \ . \qquad (25b)$$

Setting $\ddot{\epsilon} = 0$,

$$\dot{\epsilon} \left[-\beta P_n \frac{d\Delta V/V}{dt} - \frac{2}{\epsilon} \frac{d\epsilon}{dt} \right] = 0 .$$

Neglecting the solution when $\dot{\epsilon} = 0$, which only occurs when there is no shear stress applied,

$$-\beta P_n \frac{d\Delta V/V}{dt} = \frac{2}{\epsilon} \frac{d\epsilon}{dt} \tag{26}$$

at the point of inflection.

Since increasing volume has been considered as positive throughout the derivation, equation 26 shows that the slope of the volume change-time curve must be negative, and the slope must be equal to $\frac{-2}{\beta P_n \epsilon} \frac{d\epsilon}{dt}$ at the point of inflection.

Other investigators (Best and Hoover, 1966; Ferguson and Hoover, 1968) have proposed a failure criterion based on volume change measurements in constant rate-of-deformation triaxial compression tests. The condition chosen by these investigators to indicate failure is "...the minimum volume condition, or some point near this condition...."

It would be desirable to compare this failure criterion with that proposed in this investigation, especially since equation 26 indicates that the $\ddot{\epsilon} = 0$ criterion is related to the rate of volume change. The minimum volume criterion implied a zero rate of volume change ($\frac{d\Delta V/V}{dt} = 0$), but this cannot be substituted into equation 26 because in constant rate-of-deformation testing, τ is not independent of time as it is in constant load tests. Therefore, it is not possible to make a direct comparison of these two failure criteria. It is perhaps significant, however, that both are related to the rate of volume change, one requiring the rate of volume change to be negative, the other specifying a zero rate of volume

change.

Verification of any relationship between these failure criteria will await a further understanding of the mechanisms of material behavior when subjected to different test conditions. This discussion has indicated that the empirical relationship of equation 23 is not, nor does it imply conditions which are, contrary to any basic principles or the energy barrier concept of shear strength.

Consolidation pressure

As stated previously, a relationship in a form similar to that of equation 17 is desirable for evaluating the parameters ΔH^* and β and these parameters can be evaluated from that equation, provided that all other variables which affect the deformation rate or the value of these parameters are held constant.

Experimentally, however, it has been found that the rate of deformation also varies with normal stress (P_n), temperature of consolidation (T_c) (distinct from the temperature at which the deformation occurs, designated T_s, and consolidation pressure, P_c.

The effect of normal stress on the deformation rate has been shown in equation 8, which also includes part of the time-dependent structure changes which take place during the deformation of the material. However, at the point of inflection, the structure is constant for any normal stress as has been shown previously. The effect of normal pressure can be separated from the pre-exponential coefficient of equation 17 without changing the fact that the point of inflection represents a point where the effect due to structure is constant.

$$\dot{\epsilon} = C''' \exp - \frac{\Delta H^*}{kT} \exp \beta \tau \exp - \beta P_n \frac{\Delta V}{V} . \qquad (27)$$

The coefficient, C''' in equation 27 now represents, in addition to the proportionality constant and the entropy of activation, that part of the resistance to deformation due to structure changes, other than that due to $P_n \frac{\Delta V}{V}$. As such, C''' is a quantity which varies with $P_n \frac{\Delta V}{V}$, but a constant value of these effects can be evaluated by extrapolating equation 27 to zero P_n.

The effect due to consolidation pressure can be envisioned by considering the concepts of frictional resistance of solids proposed by Bowden and Tabor (1950). The actual area of contact between solids is very small compared to the total area and the area of contact is related to the applied load on the contact area. When compared to molecular dimensions, the surfaces of solids are relatively rough and the load is carried by the highest points of irregularity on the surfaces. The stresses at such contacts cause elastic and plastic deformations of the material until the contact area is large enough to carry the load.

If the applied load causes plastic deformations, bonds may form between the solid surfaces. If the release of the load allows elastic rebound sufficient to break any bonds which may have formed, no permanent adhesion between the solid particles results. In granular materials, this probably occurs and there is no frictional resistance under zero normal load. However, in clays, bonds probably form between adsorbed water layers adjacent to the surfaces (rather than between atoms of the particle surfaces) and these bonds are not all broken when the load is released. This

effect would also be present in granular materials which contain some percentage of clay or clay-size particles. In granular materials which contain no clay particles, the consolidating pressure may have an effect since the greater the normal load, the greater would be the plastic deformations of the irregular solid surfaces. This would bring the surfaces closer to each other, allowing more bonds to form between the adsorbed water on these surfaces. Also, since the plastic deformation of the irregular solid surface is itself time-dependent, the formation of such bonds would also be time dependent, and a consolidating pressure, applied for some period of time would have an effect on the number of bonds between particles. These bonds between larger particles of a granular system would probably be broken by elastic rebound if the consolidation pressure were released. If this were done prior to the application of shear stress, the effect of consolidation pressure on the rate of deformation would be negligible. Since the materials used in this investigation contained some clay particles and the consolidation pressure was not released prior to the application of the shear stress, the effect due to consolidation pressure must be included in the rate equation.

The effect of consolidation pressure on activation energy can be represented by $-\gamma' P_c$, γ' representing the decrease in the volume of an average flow unit due to the application of a consolidation pressure.

Consolidation temperature

The effect of consolidation temperature on the rate of deformation has previously been reported by Noble (1968), and was assumed to cause an exponential variation in the rate of deformation. Noble's experimental data

fit that assumption satisfactorily.

Campanella and Mitchell (1968) have shown that increasing consolidation temperature causes a decrease in void ratio for any consolidating pressure. The increase in amount of consolidation is probably due to the decreasing viscosity of water with increasing consolidation temperature. The decreased void ratio also indicates that water content is less, making the remaining adsorbed water layers thinner, thus bringing particle surfaces closer to each other. This allows more bonds to form between these thinner adsorbed water layers than between thicker adsorbed layers resulting from lower consolidation temperatures.

If the increased number of bonds per degree of consolidation temperature is represented by α', the effect of consolidation temperature can be represented by $-\alpha' T_c$.

Setting $\gamma = \frac{\gamma'}{kT}$ and $\alpha = \frac{\alpha'}{kT}$, the rate equation becomes with the inclusion of these effects of T_c and P_c;

$$\dot{\epsilon} = C'' \exp -\frac{\Delta H^*}{kT_s} \exp \beta\tau \exp -\beta P_n \frac{\Delta V}{V} \exp -\gamma P_c \exp -\alpha T_c \qquad (28)$$

where

C'' is the same as C''' but with the effects of T_c and P_c separated.

These effects of consolidation temperature and pressure are such that, at least in experimental manifestation, they change the height of the energy barrier of the material. Increased consolidation pressure increases the number of bonds, as does higher consolidation temperature, thus reducing the flow unit size, β'. Inclusion of these effects in the rate equation allows comparison of the parameter β among material specimens subjected to different values of P_c and T_c.

Model equation

The information derived from triaxial shear test data is more readily expressed in terms of principal and/or deviator stresses rather than shear and normal stresses. The major principal stress applied on a circular section of the cylindrical specimen, i.e. perpendicular to the longitudinal axis, is the confining pressure in the triaxial cell plus the deviator stress applied through the loading piston, if the effect of cell pressure on the loading piston is neglected.

$$\sigma_1 = p + \frac{L}{A} \tag{29}$$

where

σ_1 is the major principal stress,

p is the cell pressure,

L is the applied force on the loading piston, and

A is the cross-sectional area of the specimen on which the load is applied.

The minor principal stress, or the stress on any plane perpendicular to the major principal stress, is simply the cell pressure.

$$\sigma_3 = p \tag{30}$$

From Mohr stress theory, the maximum shear stress in the specimen is

$$\tau = \frac{\sigma_1 - \sigma_3}{2} \tag{31}$$

and the stress normal to the maximum shear stress is

$$p_n = \frac{\sigma_1 + \sigma_3}{2} \quad . \tag{32}$$

Substituting the relationships from equations 29 and 30 into equations 31 and 32,

$$\tau = \frac{L}{2A} \tag{33}$$

and

$$P_n = \frac{L}{2A} + p. \tag{34}$$

The consolidation pressure on any plane in the specimen is equal to the cell pressure since the specimen is isotropically stressed during consolidation in a triaxial cell.

$$P_c = p. \tag{35}$$

Substituting the relationships from equations 33, 34 and 35 into equation 28 and combining terms,

$$\dot{\epsilon} = C'' \exp - \frac{\Delta H^*}{kT_s} \exp \frac{\beta L}{2A}(1 - \Delta V/V) \exp -(\beta \Delta V/V + \gamma) p \exp - \alpha T_c. \tag{36}$$

The effect of $\Delta V/V$ on the term $\frac{\beta L}{2A}(1 - \Delta V/V)$ can be neglected since the value of $\Delta V/V$ is small compared to 1, usually less than 0.02.

Because of the nature of the triaxial test and the experimental techniques used in this investigation, the effects of P_c and P_n on the rate of deformation are inextricably interrelated. It has been found experimentally, that the effect of the variation of the pre-exponential coefficient due to structural changes and the effects of $(\beta \Delta V/V + \gamma)$ can be combined into a new linear coefficient of cell pressure, p. This coefficient, designated μ, is theoretically a variable quantity dependent on ΔV, and is probably also dependent on other quantities, but the analysis of experimental data has indicated that the consideration of μ as a constant does not introduce serious error.

Substitution of these approximations into equation 36 give the relationship:

$$\dot{\epsilon} = C' \exp - \frac{\Delta H^*}{kT_s} \exp \frac{\beta L}{2A} \exp -\mu p \exp -\alpha T_c \qquad (37)$$

which is the model equation proposed for the deformation of materials.

As can be seen from equation 34 the normal stress on the shear plane is greater than the consolidation pressure. This increase in normal stress during shear could also have an effect on the number of bonds, similar to that discussed for consolidation pressure. However, formation of bonds is time dependent and, since in this investigation the deviator stress was repetitively applied and released, there was probably insufficient time for permanent bonds to form due to the increase in P_n. If any bonds were formed, they were probably broken by elastic rebound as the deviator stress was released.

The application of deviator stress, thus increasing the normal stress, would also cause elastic deformation of the particles. Since the elastic deformation would occur on the surface irregularities, the amount of volume change necessary to allow the material to deform would increase, i.e. increased micro-dilation. The necessary increase in volume change has been included in the $\Delta V/V$ term, but to some degree, ΔV is a function of P_n. Because of this interdependence and the relationship between normal stress and consolidation stress, these effects have been combined into an experimentally determined coefficient μ in equation 37.

Equation 37 can be used to evaluate the parameters which characterize the material. If information about the total deformation or the time to reach a given total deformation is desired, equation 24 must be used.

Substituting the relationships for shear and normal stress into equation 24, neglecting the effect of $\Delta V/V$ on β as before, and including the effects of consolidation temperature and pressure, the relationship for

total strain becomes:

$$\epsilon^3 = M'' \exp -\frac{\Delta H^*}{kT_s} \exp \frac{\beta L}{2A} \exp -\mu p \exp -\alpha T_c \cdot t \qquad (38)$$

Solving this equation for t,

$$t = \frac{\epsilon^3}{M''} \exp \frac{\Delta H^*}{kT_s} \exp -\frac{\beta L}{2A} \exp \mu p \quad \exp \alpha T_c \ . \qquad (39)$$

Equation 39 can be evaluated for t at any constant ϵ, by writing

$$t_\epsilon = M' \exp \frac{\Delta H^*}{kT_s} \exp -\frac{\beta L}{2A} \exp \mu p \quad \exp \alpha T_c \qquad (40)$$

where the coefficient, M', now represents the effect of all quantities which affect the time to reach a total deformation, ϵ, which are not otherwise included in equation 40. In order to use equation 40 in this form, the quantities not specifically considered, i.e. total strain, must be held constant.

In the development of the theory to this point, the rate of deformation considered has been the time rate of shear deformation. Shear deformations in a triaxial compression test cannot be measured because of the inability to control either the shear plane or the thickness of the shear zone. It is assumed that the shear deformations are proportional to axial deformations, conveniently expressed as a percentage of the initial specimen height. Since the number of applications of deviator stress were measured rather than time, wherever time has been used as a variable it can be replaced by the number of applications divided by the frequency of applications as shown in equation 2.

The rate of deformation then becomes the rate of axial deformation per application of deviator stress if the frequency of application is included in the pre-exponential coefficient. Frequency of application was held

constant throughout this investigation. Dimensionally, this rate of deformation is in units of percent per application. Likewise, the time to reach a given deformation in equation 40 can be replaced by $\frac{N}{f}$ and the constant frequency included in that pre-exponential coefficient.

These exponential relationships can be conveniently expressed by taking logarithms of both sides of the equations. Equation 37 then becomes,

$$\ln\dot{\epsilon} = \ln C - \frac{\Delta H^*}{kT_s} + \frac{\beta L}{2A} - \mu p - \alpha T_c \qquad (41)$$

and equation 40 becomes,

$$\ln N_\epsilon = \ln M + \frac{\Delta H^*}{kT_s} - \frac{\beta L}{2A} + \mu p + \alpha T_c . \qquad (42)$$

where the coefficients C and M now include, in addition to those factors stated previously, the proportionality constants for the relationships between shear and axial deformations, the frequency of load applications and the conversion of strain to percent strain.

Equations 41 and 42 are the basic relationships which are evaluated in this investigation. Their development has been based on rate process theory and consideration of those factors known to affect the deformation rate. As will be demonstrated, they are in substantial agreement with observed experimental results.

EXPERIMENTAL PROGRAM

Material properties

The granular material used in the experimental program was a crushed dolomite obtained from a quarry near Garner, Hancock County, Iowa. The material is approved by the Iowa State Highway Commission for rolled stone bases and was tested in the condition as received from the quarry stockpile, that is, the physical and chemical properties of the crushed stone were not altered after receipt.

Material properties, as determined by standard procedures, are summarized in Table 1.

The granular material was tested both with and without stabilizing additives. The stabilizing agent used was a 120-150 penetration grade asphalt cement meeting the specifications of the Iowa State Highway Commission (1964) for petroleum asphalt.

Specimen preparation

All specimens were prepared by vibratory compaction procedures found by previous studies (Hoover, 1967) to be more suitable than other methods for preparing triaxial test specimens of granular material. Each specimen was compacted in a four-inch diameter by eight-inch high cylindrical mold attached to a Syntron Electric Vibrator table. A constant frequency of 3600 cycles per minute, amplitude of 0.368 mm, surcharge weight of 35 pounds and compaction period of two minutes, a combination of factors capable of producing standard AASHO density with a minimum amount of degradation (Hoover, 1967), were used throughout the experimental program.

Table 1. Material properties

Textural composition	
Gravel (greater than 2.0 mm)	61.6%
Sand (2.0 mm - 0.074 mm)	26.0%
Silt (0.074 mm - 0.005 mm)	10.2%
Clay (less than 0.005 mm)	2.2%
Colloids (less than 0.001 mm)	1.4%
Atterberg limits	Non-plastic
Mineralogical composition (by X-ray diffraction)	Calcite Dolomite with small amounts of Quartz Mica Kaolinite
Calcite/Dolomite ratio (by X-ray diffraction peak intensity)	1.16:1
Moisture-density relationships	
Standard AASHO-ASTM density	140.5 pcf
Standard AASHO-ASTM optimum moisture content	7.6%
Modified AASHO-ASTM density	147.6 pcf
Modified AASHO-ASTM optimum moisture content	5.4%
Specific gravity (of minus No. 10 fraction)	2.83
Textural classification	Gravelly sandy loam
AASHO classification	A-1-a

Untreated specimens were prepared by obtaining sufficient air dry material for a four-inch diameter by eight-inch high cylindrical specimen; distilled water was added to obtain optimum moisture content. The granular material and water were mixed by hand to reduce degradation of the material, after which the mixture was allowed to stand in a moist atmosphere for ten

minutes. After standing, the material was again hand mixed and two moisture samples of approximately 100-125 grams each were removed. The material was placed in the mold in three approximately equal layers, each layer being rodded 25 times with a 5/8-inch diameter tapered point steel rod.

After compaction, the height of each specimen was measured while still in the mold. The specimen was then extruded with a hydraulic jack, wrapped in two layers of Saran wrap and aluminum foil and the ends sealed. When wrapped and sealed, the specimens were encased in a plastic sleeve to prevent deformation of the specimen under its own weight and stored in a room maintained at near 75 degrees and 100 percent relative humidity until tested.

The asphalt treated specimens were prepared by obtaining sufficient aggregate and asphalt cement for the desired asphalt content (nominally 4 percent by weight of the aggregate) for each specimen. The aggregate, asphalt cement, mixing bowl and mold were heated in an oven to 250 degrees F. The aggregate and asphalt were then mixed in a mechanical mixer (Hobart Model S-601) for a period of two minutes. The mixture was again placed in the oven and maintained until the temperature of the mix reached 250 degrees F. The aggregate-asphalt mixture was then placed in a pre-heated mold and compacted in the same manner as the untreated specimens.

The asphalt content of each specimen was determined by the actual weight of asphalt cement added to the aggregate.

After compaction, the specimens were extruded from the mold and al-

lowed to cool to room temperature. They were then weighed, measured and stored at room temperature and humidity until tested.

Triaxial compression apparatus

The repetitive-load triaxial compression apparatus was designed by the Iowa State University Soil Research Laboratory and fabricated by the I.S.U. Engineering Shop and Soil Research Laboratory (Figures 4 and 5).

The axial loading system, program control center, timer, counter and necessary control valves and pressure switches were manufactured by Enerpac. The hydraulic actuator has a capacity of 17,700 pounds at 10,000 psi fluid pressure.

Applied axial load was measured by a Dillon Series 200, 10,000 pound capacity lead cell and Dillon Type B meter readout. The meter readout was calibrated to read directly in pounds, each scale division representing 50 pounds.

The timer, which controls the length of time that a preset load is held on the specimen, has a range from approximately 0.05 second to 1.0 second. The counter is capable of recording one million applications of load.

Positive and negative pore water pressureswere measured with a 0-100 psia pressure transducer (No. 4-312-0001) manufactured by Consolidated Electrodynamics and read by means of a Daytronic Corporation Model 300D Amplifier-Indicator with a Type 93 strain gauge input module. The indicator was calibrated to read directly in pounds per square inch with an arbitrary zero reference taken at atmospheric pressure. On the 10% scale,

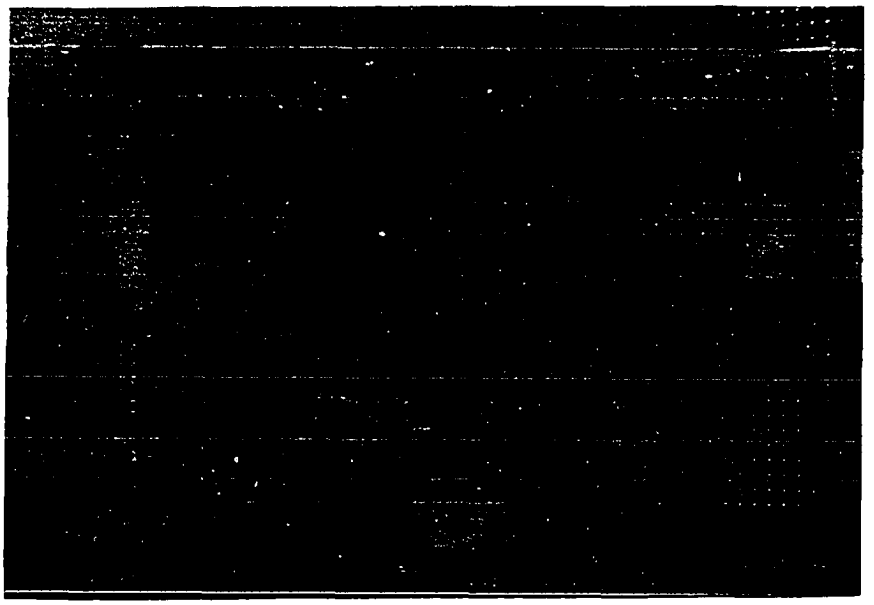

Figure 4. Repetitive load triaxial compression apparatus and control panel

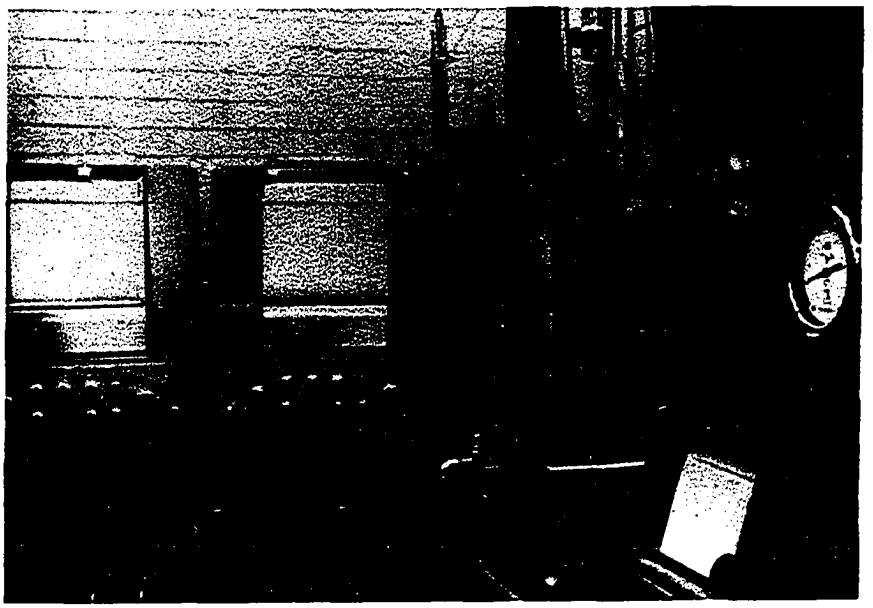

Figure 5. Repetitive load triaxial compression apparatus and strip chart recorders

each division on the indicator scale represented 0.1 psi.

Volume change measurements were made with a device developed at the Soil Research Laboratory, which incorporates a linear variable differential transformer (LVDT). This device is capable of a measurement precision near 0.03 cubic inch. Vertical deformations of the specimens were measured by a dial extensometer (0.001 inch per division) and simultaneously by an LVDT which was capable of 0.003 inch precision. Both the LVDT used in deflection measurement and that used in the volume change device were manufactured by Schaevitz Engineering.

The volume change, deflection, pore pressure and axial load measurement devices were designed and/or specified to be such that all measurements could be continuously recorded on strip-chart recorders.

Temperature control of the specimens was achieved by a controlled temperature water bath consisting of an 0.7 cubic foot insulated glass jar heated by means of an immersion heater and immersed light bulbs equipped with rheostats. The light bulbs operated intermittently by means of an immersion controller, while the immersion heater operated continuously. The temperature of the test specimen and the water in the triaxial cell were controlled by circulating water from the controlled temperature bath through a closed coil in the triaxial cell. Temperature of the cell water was measured by submerged thermocouple wires which were led through a sealed connection in the triaxial cell cap and connected to a potentiometer calibrated to read directly in degrees Centigrade. Control of the temperature of the specimen with variations less than one degree Centigrade were possible with this arrangement.

Test procedure

When ready for testing, a specimen was removed from the storage room, unwrapped, weighed and measured prior to being placed in the triaxial cell. Saturated corundum porous stones, each ½-inch thick were placed at the top and bottom of the specimen. Specimen, cap, stones and base were sealed in a 0.025-inch thick, seamless rubber membrane. The removable heating coil was placed around the specimen and the cell filled with water.

Water from the controlled temperature water bath was circulated through the closed heating coil until the thermocouple readout indicated the desired consolidation temperature. Because the temperature measured was that of the water in the cell rather than that of the specimen itself, the consolidation temperature was maintained for one hour in order to insure constant temperature throughout the system prior to application of the consolidating pressure.

In all tests, shear temperature was equal to or less than the consolidation temperature. This was necessary since any increase in temperature above consolidation temperature would result in further consolidation, and the shear strength would increase as a result of this additional consolidation. Therefore, in order to determine the effect of shear temperature separate from the consolidation temperature, the specimens in each test series were all consolidated at a temperature equal to the highest shear temperature used in the respective test series.

After equilibrating at the consolidation temperature for one hour, the consolidating pressure was applied and volume change, pore pressure and

deflection measurements recorded. A uniform consolidation period of 36 minutes was used for each specimen. With this consolidation period, all specimens reached a virtually constant volume condition.

If the shear temperature was to be equal to the consolidation temperature, the specimen drain was closed and the repetitive load process initiated immediately following consolidation. If a shear temperature lower than consolidation temperature was necessary, the specimen was cooled to the desired shear temperature. A minimum equilibration period of one hour was again used at this point in the test procedure. Cooling the specimen to the desired shear temperature after consolidating at a higher temperature is a step in the testing procedure which introduces some uncontrollable variation in the specimen, the effects of which will be discussed later.

After equilibrating at the shear temperature, the specimen drain was closed and the repetitive load process initiated. The specimens were subjected to repeated applications of a preset deviator stress until axial deformation reached approximately 15 percent of the initial specimen height or until a minimum of ten thousand applications of the stress had been sustained, which ever occurred first.

During repeated loading, pore pressure, volume change and deflection were continuously recorded on strip-chart recorders. The number of applications registered on the counter were periodically recorded on the strip-charts, thus relating pore pressure, volume change and deflection to the number of stress applications. Since deviator stress and shear temperature were held constant throughout the test period on any one specimen, these

were monitored on their respective readouts to insure that they did remain constant, but were not continuously recorded.

The dwell time, or the time that the deviator stress was maintained on the specimen during one stress application, was maintained constant at one second throughout the entire experimental program. The rise and decay times of the stress pulse, plus the "dead" time, occupied a combined total time of approximately one second so that the frequency of stress application was 30 to 33 applications per minute.

Computations necessary for the analysis of data obtained from this study were done primarily with the facilities of the Computation Center, Iowa State University, using programs especially developed by the Soil Research Laboratory.

Discussion of procedure

Despite efforts to standardize all procedures as described above, some scatter of results was observed. In a complex testing program, the large number of variable quantities comprise many potential sources of experimental error. Much of the scatter in results undoubtedly reflect these random errors.

One source of error which may well be systematic, however, involves those changes which occur in the specimen when it is cooled after having been consolidated at a higher temperature.

More consolidation takes place at higher than at lower temperatures due to the lower viscosity of water, as previously discussed. When consolidation is complete, it is impossible to lower the temperature in the

triaxial cell while maintaining the same conditions of pore pressure, moisture content and saturation. This is due to the fact that the coefficient of volumetric expansion of water is on the order of 10 times that of mineral matter. Thus, as the specimen is cooled, negative pressure occurs in the pore water as the water contracts more than the mineral matter. If the specimen is cooled with the specimen drain closed, negative pore pressures develop, the magnitude depending on the temperature differential. If the specimen is cooled with the specimen drain open, negative pore pressure will not build up, but the moisture or air content will be changed, depending on whether or not the specimen drain is connected to a water reservoir. When the drain is not connected to a water reservoir, not only will the degree of saturation be changed but the moisture distribution in the specimen will also be changed since air could enter the specimen only from one end.

Initially, all methods described above were tried in an attempt to determine a method which would give consistent results. Cooling the specimens with the drain open to a water reservoir was adopted and it was thought that changes in moisture content due to cooling the specimen would not significantly affect results. Analysis of data obtained subsequently indicates that these changes in moisture content affect the rate of deformation, that changes in moisture content should be measured, and their effect on deformation rate experimentally determined. These effects will be further discussed in the analysis of results section.

Testing program

The laboratory tests performed in this investigation were all isotropically consolidated, undrained, repetitive-load triaxial compression tests. For simplicity in discussing the results of these tests, they have been classified into series and groups according to the triaxial cell pressure and consolidation temperature as shown in Table 2. Each test is considered to consist of two stages: a consolidation phase, in which the specimen was isotropically consolidated under a cell pressure equal to the confining pressure on the specimen during shear; and a triaxial shear phase during which a deviator stress was repeatedly applied and released from the specimen. Each test group consists of several specimens differing only in the level of repeatedly applied deviator stress.

Table 2. Test series and groups

Series	Group	P_c, psi	T_c, °C	T_s, °C
A	5A	5	25	25
	10A	10	25	25
	15A	15	25	25
	20A	20	25	25
B1	25B1	10	60	25
	40B1	10	60	40
	60B1	10	60	60
B2	25B2	20	60	25
	40B2	20	60	40
	60B2	20	60	60
6	25C	10	60	25
	40C	10	60	40
	60C	10	60	60

In Table 2, P_c is consolidation pressure and T_c and T_s are consolidation and shear temperature respectively. Test series A consists of all untreated specimens consolidated and sheared at 25 degrees C. Test groups in series A designate the consolidation pressure for that group. Test series B1 and B2 consolidated at 60°C, series B1 having been consolidated and sheared under 10 psi pressure and series B2 under 20 psi pressure. Test series C consists of asphalt treated specimens, all consolidated at 60°C and sheared under 10 psi pressure. The test groups in Series B1, B2 and C indicate the shear temperature.

RESULTS AND ANALYSIS

Methods of analysis

Small variations in materials, specimen preparation, and testing procedure are reflected in the behavior of each specimen. Since each test and/or group or series of tests contained a reasonable number of data points, and the equations describing material behavior (equations 18, 41, and 42) consist of linear relationships or combinations of linear relationships, the data could be treated by least squares fitting. All data have been so treated and the results are discussed subsequently. Statistical tests, where appropriate have been made on the quantities thus computed as an aid in interpreting the results.

Because of the number of tests and the number of individual data points obtained for each test, it is not practical to include all of the primary data from all tests in either tabular or graphical form, but tables of observed quantities and representative graphs have been included for each type of analysis.

Since pore pressure does not appear in any of the equations proposed to describe material behavior, no attempt has been made to describe the effect of pore pressure on the rate of deformation. This is not to say that pore pressure does not affect the material behavior but rather that pore pressure does not independently affect the material behavior, and any such effect has been included in other quantities. The pore pressure measurements and the deflection measurements made with the dial gauge extensometer were a useful means of observing the general behavior of the specimen at any stage during a test.

Strain-stress application relationships

The total strain after various numbers of stress applications were computed. Typical plots are shown in Figures 6 and 7 for Test Groups 10A and 25C. These curves show the effect of different deviator stresses at fixed levels of other variables. The shape of these curves is essentially the same as those published by other researchers for soils and other materials is the number of applications were to be replaced by time in the abscissa.

To test the applicability of equation 18 to the deformation of material, plots of strain versus the cube root of the number of applications were made and are shown typically in Figures 8 and 9. Least squares regression analysis of all 64 tests are shown in Tables 3 through 15. Deviator stress (equal to $\frac{L}{A}$ in equation 33) is denoted D, ϵ is the axial strain and N is the number of applications of the designated deviator stress. Columns headed ϵ_o and b indicate values of intercept and slope computed in the regression analysis, and below each value, its standard error. The column headed r is the correlation coefficient of the regression. It is emphasized that these analyses do not represent the entire strain versus stress application curve; only the transient portion of the creep curve is represented (stage II of Figure 3).

Computed values of "b" in Tables 3 through 15 reflect the changing value of deviator stress. Apparently volume change of the specimen is, in the range of strain considered here, also a linear function of deviator stress so that this effect is included in the computed value of "b". At

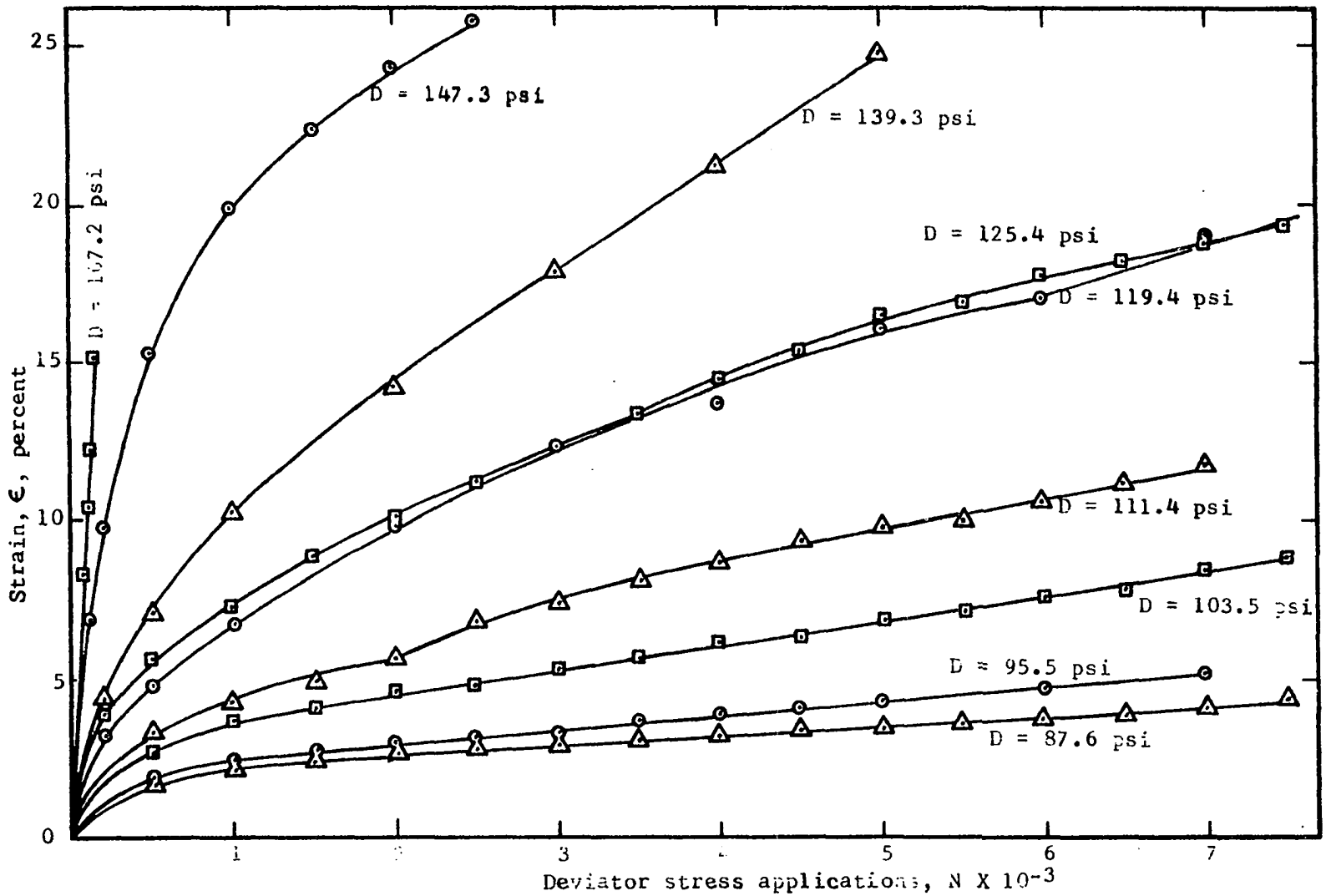

Figure 6. Strain versus deviator stress applications curves, Group 10A

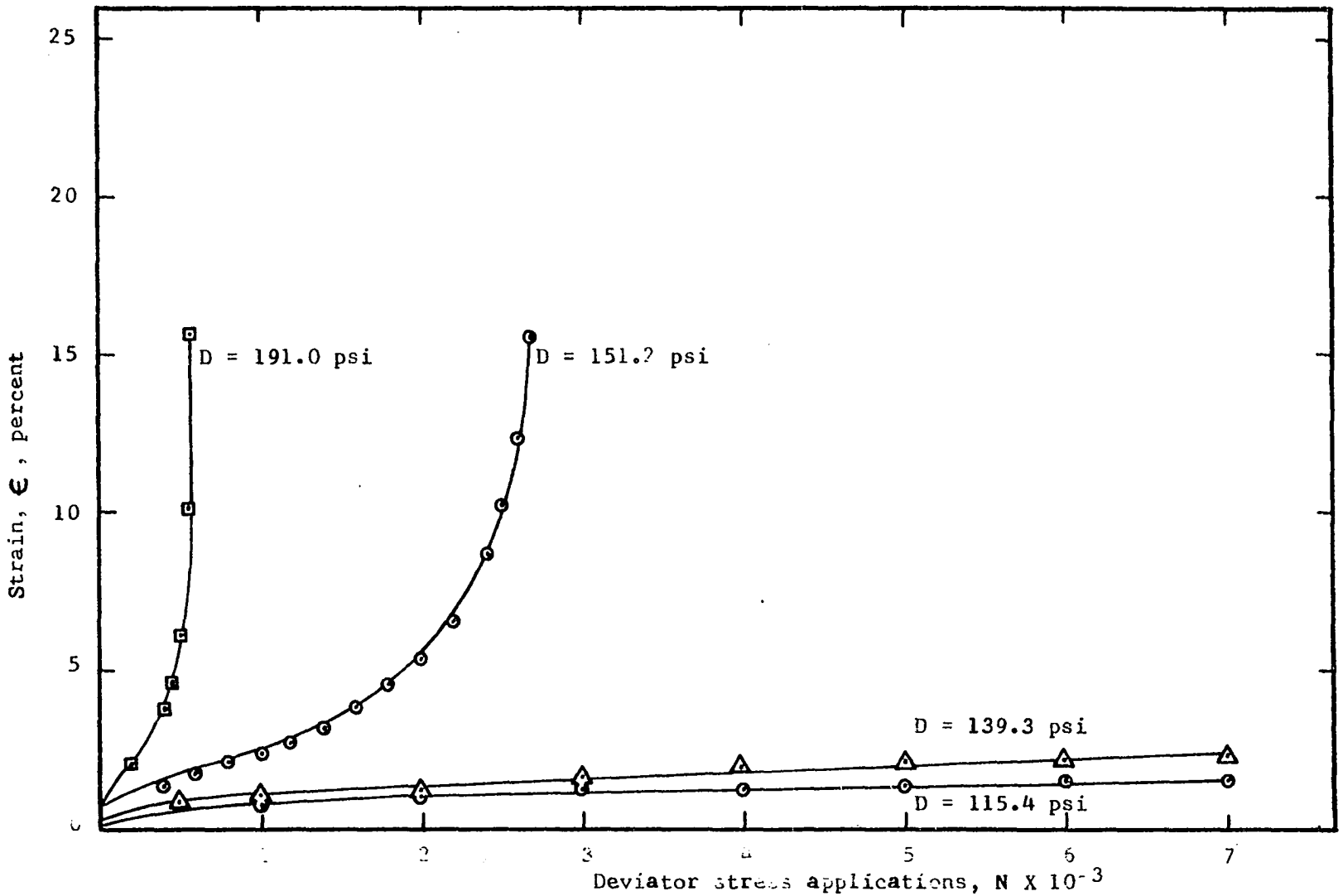

Figure 7. Strain versus deviator stress applications curves, Group 25C

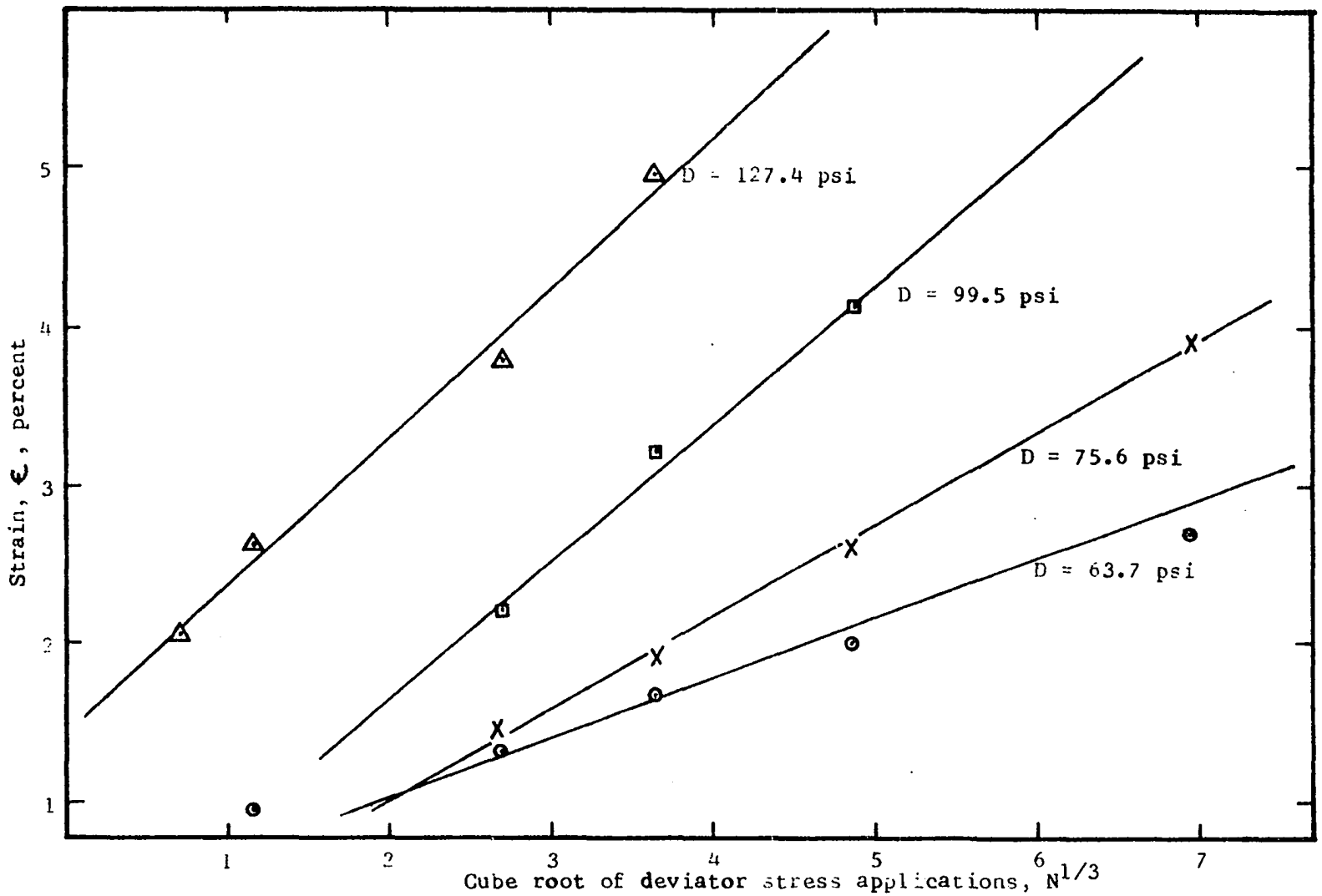

Figure 5. Strain versus cube root of deviator stress applications relationships, Group 5A

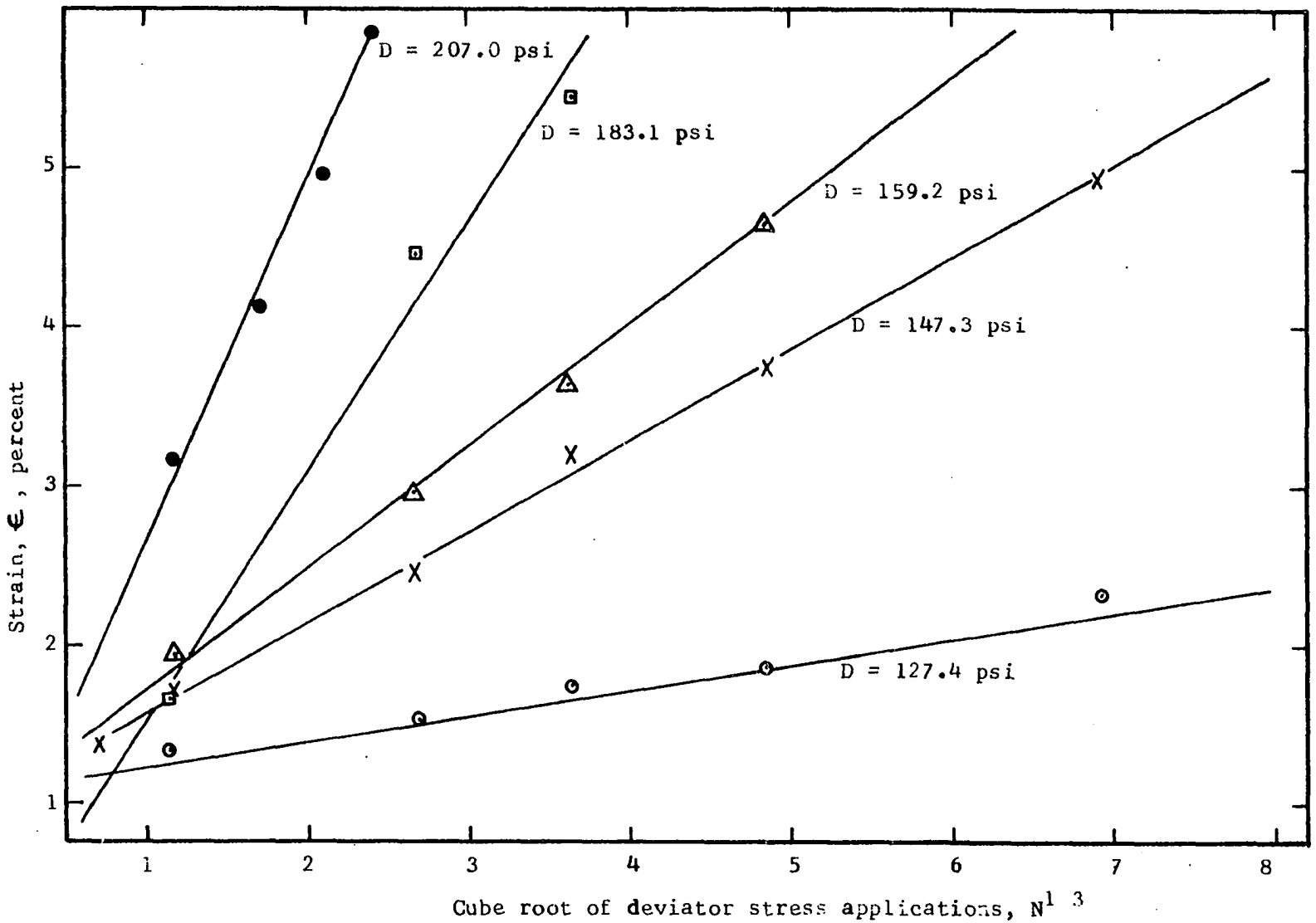

Figure 9. Strain versus cube root of deviator stress applications relationships, Group 15A

Table 3. Strain-stress applications, Group 5A

D psi	ϵ %	N	$N^{1/3}$	Regression analysis, ϵ vs $N^{1/3}$		
				ϵ_o / s_e	b / s_e	r
63.7	0.94	10	2.154	-0.099	0.377	0.997
	1.28	50	3.684			
	1.66	100	4.642	0.088	0.009	
	2.00	200	5.848			
	2.72	500	7.937			
	3.58	1000	10.000			
	4.11	1500	11.447			
	4.64	2000	12.599			
	5.13	2500	13.572			
	5.39	3000	14.422			
	5.73	3500	15.183			
75.6	1.46	50	3.684	-0.746	0.582	0.998
	1.91	100	4.642			
	2.62	200	5.848	0.117	0.021	
	3.91	500	7.937			
99.5	2.17	50	3.684	-0.991	0.880	0.999
	3.21	100	4.642			
	4.14	200	5.848	0.187	0.032	
	5.97	500	7.937			
119.4	1.83	5	1.710	-0.592	0.303	0.993
	2.06	10	2.154			
	4.00	50	3.684	0.358	0.110	
127.4	2.05	5	1.710	0.462	0.950	0.995
	2.61	10	2.154			
	3.80	50	3.684	0.207	0.063	
	4.96	100	4.642			

Table 4. Strain-stress applications, Group 10A

D psi	ϵ %	N	$N^{1/3}$	Regression analysis, ϵ vs $N^{1/3}$		
				ϵ_o s_e	b s_e	r
87.6	1.03	10	2.154	0.734	0.152	0.996
	1.41	50	3.684			
	1.45	100	4.642	0.046	0.066	
	1.60	200	5.848			
	1.91	500	7.937			
	2.32	1000	10.000			
	2.44	1500	11.447			
	2.60	2000	12.599			
	2.82	2500	13.572			
	2.98	3000	14.423			
	3.09	3500	15.183			
95.5	0.75	5	1.170	0.389	0.187	0.999
	0.81	10	2.154			
	1.07	50	3.684	0.021	0.003	
	1.24	100	4.642			
	1.45	200	5.848			
	1.85	500	7.937			
	2.25	1000	10.000			
	2.53	1500	11.447			
	2.79	2000	12.599			
103.5	1.42	50	3.684	0.010	0.360	0.998
	1.64	100	4.462			
	2.09	200	5.848	0.082	0.009	
	2.77	500	7.937			
	3.74	1000	10.000			
	4.04	1500	11.447			
	4.57	2000	12.599			
	4.91	2500	13.572			
111.4	0.75	5	1.710	-0.252	0.460	0.998
	0.78	10	2.154			
	1.27	50	3.684	0.082	0.011	
	1.75	100	4.642			
	2.42	200	5.848			
	3.39	500	7.937			
	4.36	1000	10.000			
	5.00	1500	11.447			
	5.63	2000	12.599			

Table 4. (Continued)

D psi	ϵ %	N	$N^{1/3}$	Regression analysis, ϵ vs $N^{1/3}$		
				ϵ_o s_e	b s_e	r
119.4	1.10	10	2.154	-0.052	0.632	0.993
	2.41	50	3.684			
	3.03	100	4.642	0.228	0.044	
	3.72	200	5.848			
	4.82	500	7.937			
125.4	1.58	10	2.154	0.185	0.625	0.998
	2.43	50	3.684			
	3.04	100	4.642	0.115	0.027	
	3.89	200	5.848			
139.3	1.58	10	2.154	0.031	0.703	0.996
	2.53	50	3.684			
	3.35	100	4.642	0.234	0.064	
147.3	2.43	10	2.154	-1.424	1.827	0.997
	5.51	50	3.684			
	6.93	100	4.642	0.515	0.141	
159.2	2.21	5	1.710	-0.065	1.264	0.981
	2.49	10	2.154			
	3.25	19	2.668	0.431	0.179	
	3.74	25	2.924			
167.2	1.45	1	1.000	-0.287	1.790	0.999
	1.94	2	1.260			
	2.87	5	1.710	0.068	0.032	
	3.62	10	2.154			
	4.10	15	2.466			
	4.55	20	2.714			
	4.92	25	2.924			

Table 5. Strain-stress applications, Group 15A

D psi	ϵ %	N	$N^{1/3}$	Regression analysis, ϵ vs $N^{1/3}$		
				ϵ_o s_e	b s_e	r
127.4	1.33	10	2.154	0.886	0.181	0.995
	1.52	50	3.684			
	1.75	100	4.642	0.056	0.009	
	1.86	200	5.848			
	2.32	500	7.937			
	2.74	1000	10.000			
127.4	1.88	50	3.684	1.276	0.163	0.992
	2.07	100	4.642			
	2.26	200	5.848	0.082	0.010	
	2.45	500	7.937			
	2.92	1000	10.000			
	3.20	1500	11.447			
147.3	1.38	5	1.710	0.448	0.570	0.999
	1.71	10	2.154			
	2.49	50	3.684	0.063	0.013	
	3.20	100	4.642			
	3.76	200	5.848			
	4.95	500	7.937			
159.2	10	2.154	0.181	0.181	0.770	0.998
	2.98	50	3.684			
	3.63	100	4.642	0.137	0.026	
	4.65	200	5.848			
	6.38	500	7.937			
183.1	1.66	10	2.154	-1.548	1.544	0.997
	4.46	50	3.684			
	5.44	100	4.642	0.310	0.063	
	7.41	200	5.848			
	8.84	300	6.694			
191.0	1.75	5	1.710	0.274	0.864	0.999
	2.14	10	2.154			
	3.46	50	3.684	0.013	0.005	
207.0	3.15	10	2.154	-1.872	2.256	0.997
	4.13	20	2.714			
	4.98	30	3.107	0.247	0.073	
	5.85	40	3.420			
	6.42	50	3.684			
	6.98	60	3.915			
	7.52	70	4.121			

Table 6. Strain-stress applications, Group 20A

D psi	ϵ %	N	$N^{1/3}$	Regression analysis, ϵ vs $N^{1/3}$		
				ϵ_o s_e	b s_e	r
151.2	1.66	10	2.154	0.859	0.453	0.999
	2.67	50	3.684			
	3.00	100	4.642	0.066	0.005	
	3.65	200	5.848			
	4.26	500	7.937			
	5.46	1000	10.000			
	6.07	1500	11.447			
	6.59	2000	12.599			
	6.97	2500	13.572			
	7.35	3000	14.423			
	7.76	3500	15.183			
	8.03	4000	15.874			
	8.25	4500	16.510			
	8.59	5000	17.100			
	8.97	5500	17.652			
191.0	1.48	5	1.710	0.598	0.602	0.997
	1.94	10	2.154			
	2.89	50	3.684	0.107	0.022	
	3.53	100	4.642			
	4.06	200	5.848			
	5.32	500	7.937			
207.0	3.44	50	3.684	-0.648	1.098	0.999
	4.47	100	4.642			
	5.65	200	5.848	0.185	0.032	
	8.13	500	7.937			
222.9	1.43	5	1.710	-0.449	1.101	0.999
	1.95	10	2.154			
	3.56	50	3.684	0.058	0.018	
	4.69	100	4.642			
230.8	1.60	1	1.000	-0.172	1.651	0.999
	2.57	5	1.710			
	3.28	10	2.154	0.101	0.038	
	4.29	20	2.714			
	4.92	30	3.107			
	5.53	40	3.420			
	5.97	50	3.684			

Table 7. Strain-stress applications, Group 25B1

D psi	ϵ %	N	$N^{1/3}$	Regression analysis, ϵ vs $N^{1/3}$		
				ϵ_o	b	r
				s_e	s_e	
127.4	1.71	50	3.684	0.908	0.206	0.999
	1.86	100	4.642			
	2.05	200	5.848	0.035	0.003	
	2.54	500	7.937			
	3.07	1000	10.000			
	3.19	1500	11.447			
	3.44	2000	12.599			
	3.68	2500	13.572			
	3.91	3000	14.225			
	4.02	3500	15.183			
	4.16	4000	15.874			
	4.29	4500	16.510			
	4.42	5000	17.100			
	4.56	5500	17.652			
	4.67	6000	18.171			
143.3	2.46	50	3.684	-1.883	1.179	0.999
	3.60	100	4.642			
	5.01	200	5.848	0.031	0.006	
163.2	4.07	50	3.684	1.462	0.700	0.999
	4.68	100	4.642			
	5.54	200	5.848	0.075	0.013	
	6.64	400	7.368			
191.0	3.32	10	2.154	-0.520	1.772	0.998
	4.24	20	2.714			
	5.02	30	3.107	0.264	0.098	
207.0	2.08	5	1.710	-0.591	1.533	0.998
	2.65	10	2.154			
	3.52	20	2.714	0.174	0.070	
	4.22	30	3.107			

Table 8. Strain-stress applications, Group 40B1

D psi	ϵ %	N	$N^{1/3}$	Regression analysis, ϵ vs $N^{1/3}$		
				ϵ_o	b	r
				s_e	s_e	
111.4	1.83	100	4.642	0.901	0.193	0.998
	2.02	200	5.848			
	2.40	500	7.937	0.050	0.006	
	2.82	1000	10.000			
	3.14	1500	11.447			
127.4	2.16	50	3.684	0.770	0.376	0.998
	2.47	100	4.642			
	3.02	200	5.848	0.091	0.016	
	3.74	500	7.937			
143.3	3.26	50	3.684	0.716	0.695	0.999
	3.99	100	4.642			
	4.75	200	5.848	0.081	0.014	
	6.24	500	7.937			
179.1	2.11	10	2.154	-0.776	1.325	0.999
	4.03	50	3.684			
	5.42	100	4.642	0.195	0.053	
191.0	2.54	10	2.154	-0.874	1.552	0.997
	4.67	50	3.684	0.442	0.121	
	6.44	100	4.642			
207.0	1.46	1	1.000	0.179	1.259	0.998
	1.76	2	1.260			
	2.29	5	1.710	0.077	0.048	
	2.92	10	2.154			

Table 9. Strain-stress applications, Group 60B1

D psi	ϵ %	N	$N^{1/3}$	Regression analysis, ϵ vs $N^{1/3}$ ϵ_o s_e	b s_e	r
127.4	1.71	10	2.154	1.038	0.335	0.993
	2.36	50	3.684			
	2.59	100	4.642	0.116	0.027	
	2.97	200	5.848			
127.4	1.65	10	2.154	0.981	0.310	0.997
	2.10	50	3.684			
	2.47	100	4.642	0.070	0.016	
	2.77	200	5.848			
143.3	2.35	50	3.684	0.819	0.411	0.998
	2.70	100	4.642			
	3.24	200	5.848	0.118	0.024	
163.2	4.24	50	3.648	0.598	1.012	0.998
	5.41	100	4.642			
	6.54	200	5.848	0.245	0.046	
	7.32	300	6.694			
207.0	2.78	5	1.710	-0.072	1.666	0.997
	3.54	10	2.154			
	3.96	15	2.466	0.196	0.085	
	4.49	20	2.714			

Table 10. Strain-stress applications, Group 25B2

D psi	ϵ %	N	$N^{1/3}$	Regression analysis, ϵ vs $N^{1/3}$ ϵ_o s_e	b s_e	r
183.1	2.41	50	3.684	0.873	0.431	0.998
	2.94	100	4.462			
	3.40	200	5.848	0.113	0.020	
	4.28	500	7.937			
199.0	2.56	50	3.684	-0.362	0.779	0.995
	3.16	100	4.462			
	4.23	200	5.848	0.011	0.074	
199.0	2.49	50	3.684	0.108	0.646	0.999
	3.10	100	4.642			
	3.87	200	5.848	0.355	0.002	
238.8	3.84	50	3.684	-0.771	1.248	0.999
	5.01	100	4.642			
	6.52	200	5.848	0.036	0.007	
	8.44	400	7.368			

Table 11. Strain-stress applications, Group 40B2

D psi	ϵ %	N	$N^{1/3}$	Regression analysis, ϵ vs $N^{1/3}$		
				ϵ_o	b	r
				s_e	s_e	
199.0	2.17	50	3.684	0.878	0.352	0.999
	2.52	100	4.642			
	2.94	200	5.848	0.018	0.004	
238.8	3.15	50	3.684	0.297	0.771	0.999
	3.87	100	4.642			
	4.81	200	5.848	0.047	0.010	

Table 12. Strain-stress applications, Group 60B2

D psi	ϵ %	N	$N^{1/3}$	Regression analysis, ϵ vs $N^{1/3}$		
				ϵ_o	b	r
				s_e	s_e	
183.1	2.27	50	3.684	0.604	0.454	0.999
	2.72	100	4.642			
	3.25	200	5.848	0.047	0.010	
199.0	2.41	50	3.684	0.638	0.478	-
	2.87	100	4.642	-	-	
238.8	3.31	50	3.684	0.572	0.757	0.999
	4.15	100	4.642			
	5.02	200	5.848	0.122	0.022	
	6.12	400	7.368			

Table 13. Strain-stress applications, Group 25C

D psi	ϵ %	N	$N^{1/3}$	Regression analysis, ϵ vs $N^{1/3}$		
				ϵ_o	b	r
				s_e	s_e	
115.4	0.56	50	3.684	0.315	0.080	0.953
	0.75	100	4.642	0.103		
	0.78	200	5.848		0.018	
	0.93	500	7.937			
139.3	0.55	50	3.684	0.270	0.080	0.985
	0.63	100	4.642			
	0.78	200	5.848	0.057	0.010	
	0.88	500	7.937			
151.2	0.76	50	3.684	0.176	0.121	0.909
	0.95	100	4.642			
	1.15	200	5.848	0.007	0.033	
191.0	0.55	10	2.154	-0.175	0.331	0.995
	1.00	50	3.684			
	1.34	100	4.642	0.113	0.031	

Table 14. Strain-stress applications, Group 40C

D psi	ϵ %	N	$N^{1/3}$	Regression analysis, ϵ vs $N^{1/3}$		
				ϵ_o	b	r
				s_e	s_e	
99.5	1.22	50	3.684	-0.206	0.381	0.998
	1.54	100	4.642			
	2.04	200	5.848	0.108	0.023	
111.4	1.33	50	3.684	-1.292	0.706	0.999
	1.96	100	4.642			
	2.85	200	5.848	0.119	0.025	
119.4	1.11	50	3.684	-0.379	0.397	0.994
	1.41	100	4.642			
	1.97	200	5.848	0.205	0.043	
135.3	0.95	10	2.154	0.109	0.431	0.988
	1.84	50	3.684			
	2.57	100	5.848	0.275	0.066	

Table 15. Strain-stress applications, Group 60C

D psi	ϵ %	N	$N^{1/3}$	Regression analysis, ϵ vs $N^{1/3}$		
				ϵ_o / s_e	b / s_e	r
79.6	1.00	100	4.642	-1.977	0.649	0.999
	1.86	200	5.848			
	3.16	500	7.937	0.157	0.025	
91.5	1.41	50	3.684	-2.064	0.900	0.992
	2.09	100	4.642			
	2.92	200	5.848	0.450	0.078	
	5.22	500	7.937			
99.5	2.36	50	3.684	-5.029	1.993	0.997
	4.10	100	4.642			
	5.63	150	5.313	0.595	0.129	
111.4	1.26	5	1.710	-2.903	2.278	0.975
	1.72	10	2.154			
	3.02	20	2.714	0.896	0.361	
	4.46	30	3.107			

strain values above those listed in Tables 3 through 15, volume change has an effect independent of, or at least not linearly related to, deviator stress and the strain application relationship cannot be represented beyond these values by equation 18.

Values of the intercept, ϵ_o, in Tables 3 through 15, indicate no systematic relationship to the level of deviator stress but appear to be distributed about zero. Of the 64 regression analyses, there are 30 negative values of the intercept and 34 positive values. Approximately one-half of the values of ϵ_o are not statistically significant at a significance level of 0.05.

Because of this apparent random variation in the computed values of ϵ_o, the assumption, made in writing equation 22, that the elastic deformation is small compared to the total deformation seems to be justified. Computed values of ϵ_o are thought to represent experimental variation in apparatus and procedure. Some obvious potential sources of error include imperfect contacts between various elements of the loading mechanism, and variable seating of porous stones on the ends of the specimen, when the repetitive load process was initiated.

Deviator stress-application relationships

The number of applications at which each specimen reached total strains of 2 and 5 percent were computed and plotted on a semi-logarithmic scale versus the applied deviator stress for each test group. All other variables were constant. Typical examples are shown in Figures 10 and 11. Regression analyses for all 13 groups of tests are shown in Tables 16 through 19, where the column headings are as previously defined.

The intercept, calculated by extrapolating equation 42 to zero deviator stress, has no physical significance, since it would represent the calculated number of applications of zero deviator stress necessary to produce the stipulated strain.

The values of β calculated for total strains of 2 and 5 percent exhibit some variation in some test groups. From the derivation of equation 42, the difference between the 2 and 5 percent strain curves should be constant and independent of deviator stress level. However, this derivation was based on the assumption that the effect of ϵ_o could be neglected if it is

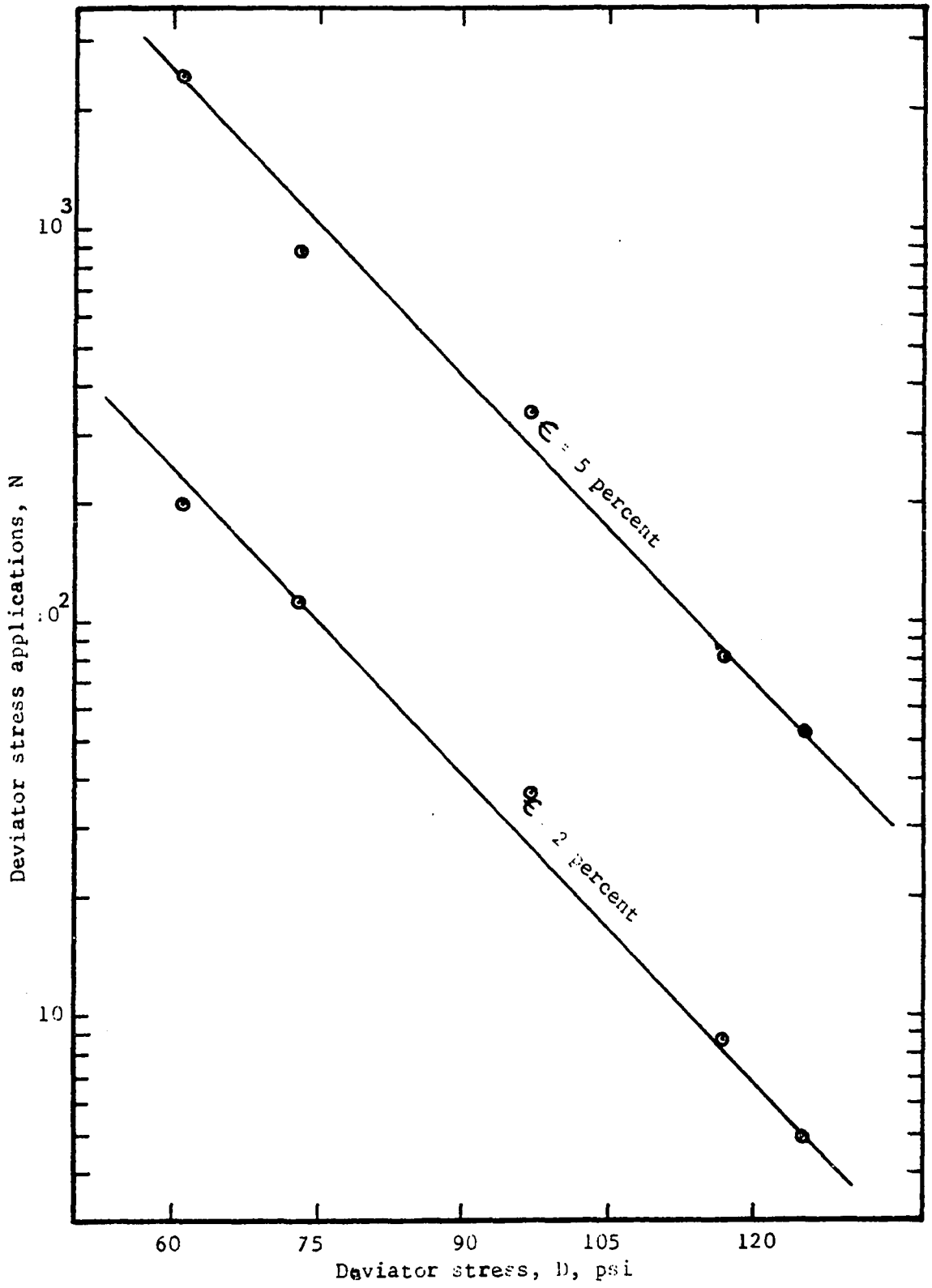

Figure 10. Variation in number of stress applications for 2 and 5 percent strain with deviator stress, Group 5A

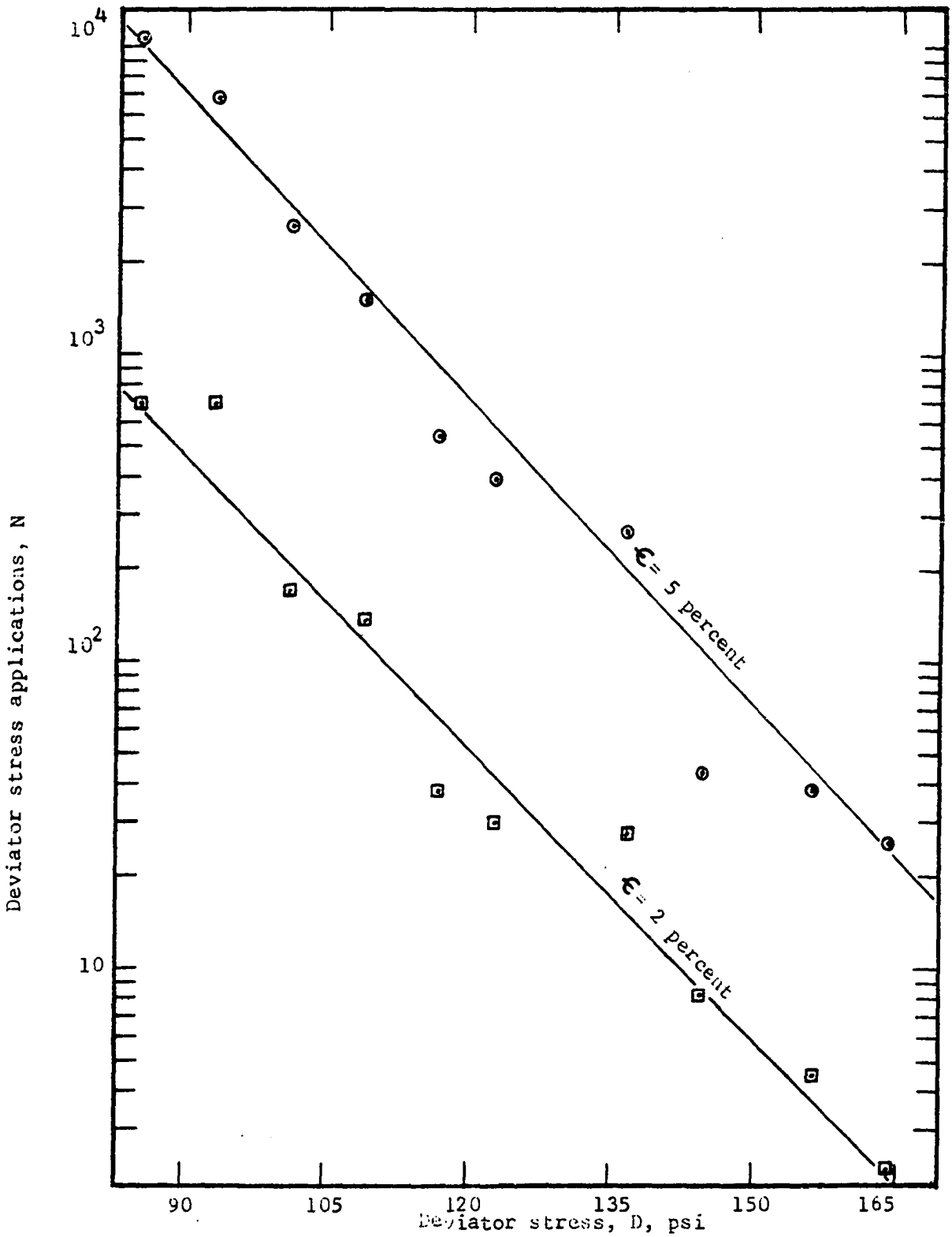

Figure 11. Variation in number of stress applications for 2 and 5 percent strain with deviator stress, Group 10A

Table 16. Stress-applications at 2 and 5 percent strain, Series A

Group	D psi	N 2%	N 5%	Regression analysis ln N_ϵ vs D					
				2%			5%		
				Intercept s_e	$\beta/2 \times 10^2$ s_e	r	Intercept s_e	$\beta/2 \times 10^2$	r
5A	63.7	200	2423	9.116	5.807	0.995	11.415	5.834	0.995
	75.6	113	877						
	99.5	37	340	0.346	0.345		0.354	0.353	
	119.4	8.6	81						
	127.4	4.9	52						
10A	87.6	698	10791	12.892	7.245	0.983	13.752	7.862	0.986
	95.5	689	6728						
	103.5	179	2593	0.619	0.483		0.595	0.464	
	111.4	137	1502						
	119.4	37	546						
	125.4	30	391						
	139.3	28	265						
	147.3	8.2	43						
	159.2	4.5	38						
	167.2	2.2	26						
15A	127.4	289	5030	9.485	3.582	0.881	16.752	6.759	0.976
	127.4	81	4977						
	147.3	25	518	1.534	0.925		1.121	0.676	
	159.2	12	260						
	183.1	15	78						
	191.0	8.2	31						
	207.0	6.3	30						
20A	151.2	23	808	6.449	2.092	0.817	12.551	3.671	0.924
	191.0	13	424						
	207.0	29	145	1.726	0.852		1.780	0.878	
	222.9	11	118						
	230.8	2.6	31						

Table 17. Stress-applications at 2 and 5 percent strain, Series B1

Group	D psi	N 2%	N 5%	Regression analysis $\ln N_\epsilon$ vs D					
				2%			5%		
				Intercept s_e	$\beta/2x10^2$ s_e	r	Intercept s_e	$\beta/2x10^2$ s_e	r
25B1	127.4	174	7921	10.538	4.459	0.983	16.015	6.351	0.922
	143.3	41	498						
	163.2	25	138	0.803	0.475		2.599	1.538	
	191.0	6.0	30						
	207.0	4.8	41						
20B1	111.4	190	4744	8.975	3.372	0.979	13.089	4.743	0.965
	127.4	46	1000						
	143.3	31	250	0.630	0.385		1.050	0.642	
	179.1	9.5	85						
	191.0	7.9	59						
	207.0	3.4	37						
60B1	127.4	28	1343	7.407	2.833	0.922	13.687	5.199	0.966
	127.4	41	1221						
	143.3	43	703	1.070	0.684		1.246	0.796	
	163.2	24	82						
	207.0	3.6	25						

Table 18. Stress-applications at 2 and 5 percent strain, Series B2

Group	D psi	N 2%	N 5%	Regression analysis $\ln N_\epsilon$ vs D					
				2%			5%		
				Intercept s_e	$\beta/2x10^2$ s_e	r	Intercept s_e	$\beta/2x10^2$ s_e	r
25B2	183.1	42	836	5.433	0.901	0.974	13.613	3.776	0.997
	199.0	39	466						
	199.0	40	405	0.305	0.148		0.389	0.189	
	238.8	26	100						
40B2	199.0	46	1536	5.645	0.885	-	16.920	4.805	-
	238.8	32	226	-	-	-	-	-	
60B2	183.1	44	1247	5.094	0.706	0.994	13.567	3.443	0.986
	199.0	41	989						
	238.8	30	198	0.156	0.075		1.195	0.574	

Table 19. Stress-applications at 2 and 5 percent strain, Series C

Group	D psi	N 2%	N 5%	Regression analysis ln N_ϵ vs D					
				2%			5%		
				Intercept	$\beta/2x10^2$	r	Intercept	$\beta/2x10^2$	r
25C	115.4	11289	-	13.305	5.495	0.963	14.890	5.878	0.919
	139.3	4380	14150						
	151.2	738	1902	1.648	1.086		4.076	2.514	
	191.0	200	462						
40C	99.5	193	912	8.029	2.741	0.721	9.990	3.221	0.849
	111.4	105	441						
	119.4	205	695	2.180	1.860		1.658	1.415	
	135.3	61	248						
60C	79.6	231	1516	12.961	9.327	0.996	17.102	12.179	0.996
	91.5	93	471						
	99.5	42	129	0.516	0.536		0.736	0.765	
	111.4	12	34						

small compared to ϵ. The general validity of this assumption has been shown in the previous section, but in some groups, especially in Series B2, the value of ϵ_o apparently has considerable effect on the calculated value of β at 2 percent strain.

Strain rate-stress relationships

A necessary condition for the valid application of equation 41 to the deformation of materials is that the value of the strain rate ($\dot{\epsilon}$), must be determined at the point where strain acceleration ($\ddot{\epsilon}$) is zero, as has been discussed previously. A method of determining the strain rate at the point where $\ddot{\epsilon} = 0$ has been reported by Noble (1968). Calculated values of strain rate were plotted versus the strain corresponding to the calculated strain rate. From these plots, points of minimum strain rate could be determined,

representing the point where $\ddot{\epsilon} = 0$. The point actually determined by this graphical method is $\frac{d\dot{\epsilon}}{d\epsilon} = 0$, but it can easily be shown that $\frac{d\dot{\epsilon}}{dt} = 0$ at the same point.

The above method of determining meaningful strain rates has been used in this investigation. Strain rate was calculated for each data point on the strain-stress application curve. Calculations were made with a computer program by taking differential strain between two data points and dividing by number of stress applications between data points. The value of strain rate thus determined was reported for the leading data point of the two considered. This method is not exact since the slope of the strain versus stress application curve is computed for an increment of the curve and reported as the strain rate at a point. However, by choosing data points at close enough intervals of stress application, the precision of the calculations can be made adequate for the intended purpose. Also, this method is believed to be as precise as, and certainly less prone to error than, any graphical method of determining strain rate at a point that might be devised.

Values of the strain rate thus determined were plotted versus the respective value of strain at which they occurred. Because of the wide range in the value of strain rate for each stress level, the curves were plotted with strain rate on a logarithmic scale. Figures 12 and 13 show these plots for Groups 10A and 25C. As can be seen in Figure 12, not all curves exhibit a definite minimum value of strain rate. Some, especially at lower stress levels, have a minimum value after which the strain rate increases and then decreases again. To determine a strain rate value corresponding

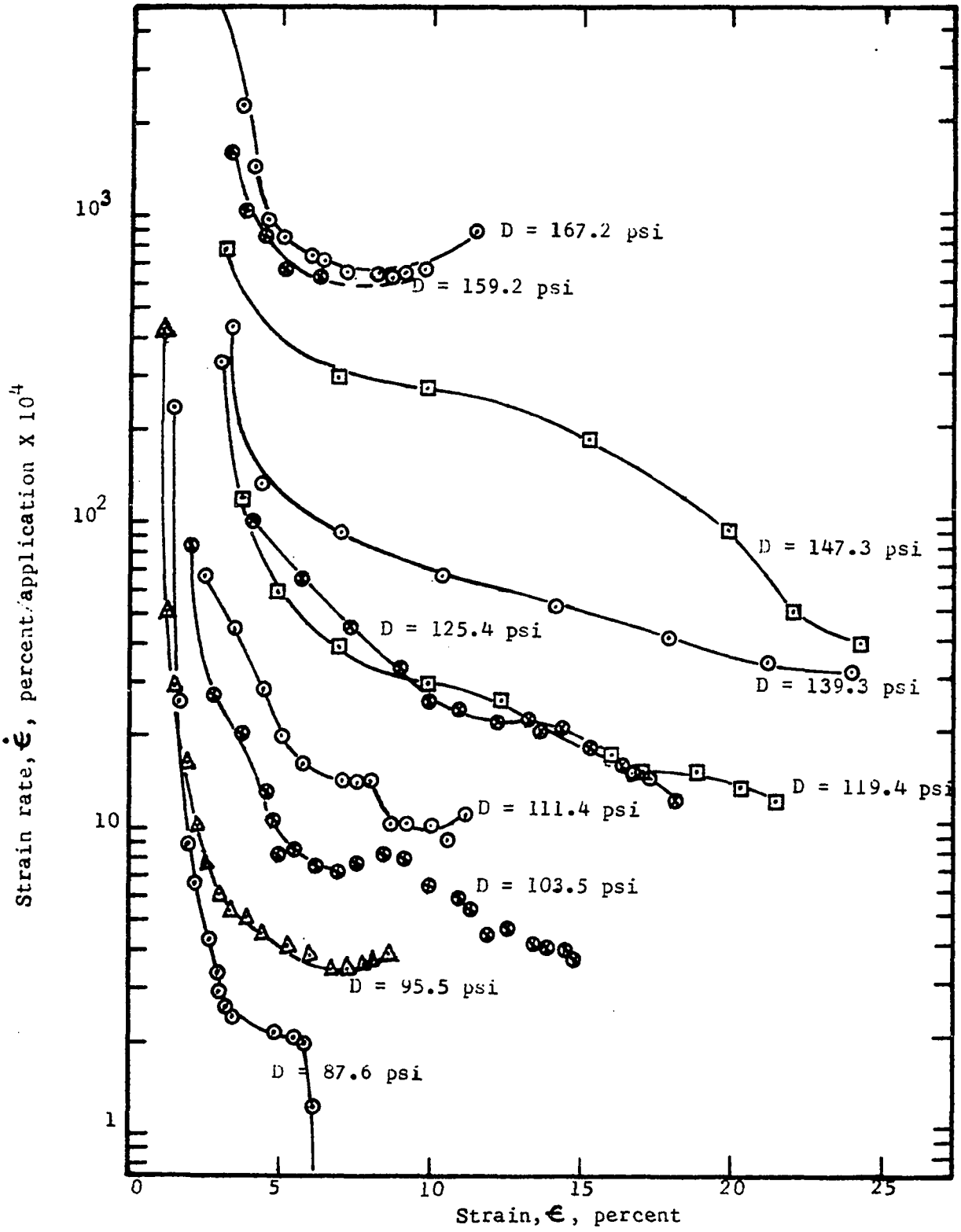

Figure 12. Strain rate versus strain, Group 10A

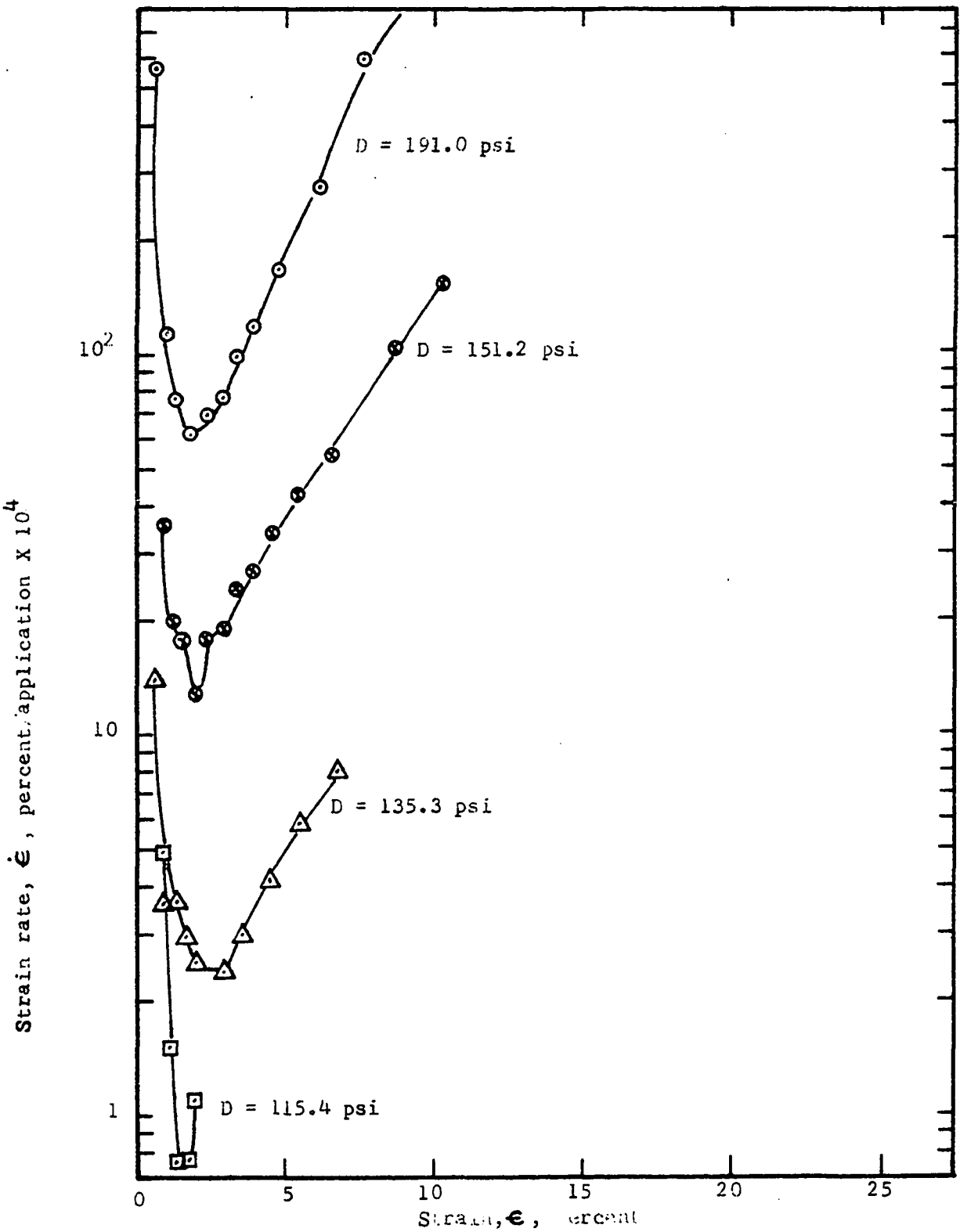

Figure 13. Strain rate versus strain, Group 25C

to $\ddot{\epsilon} = 0$ for all stress levels, a line was drawn connecting the minimum points of those curves which did exhibit minima; strain rate at the point where this line intersected those curves having no definite minimum was used as the strain rate for that respective stress level.

The phenomenon exhibited by some curves of having a minimum point followed by an increase and then further decrease in strain rate is attributed to the confinement of the specimen in the triaxial test. The increasing strain rate very likely represents incipient rupture of the material, but rupture is prevented since the specimen is confined in the triaxial cell.

Tables 20 through 23 show the values of strain rate thus determined for each stress level in all test groups. Also included in these tables are the moisture content (or asphalt content) as determined at the time each specimen was molded. Regression results shown in these tables were obtained from regression of logarithm strain rate versus deviator stress in each test group. Consolidation and shear temperatures as well as confining pressure were held constant within each test group. Moisture content or asphalt content has not been included as a variable in this analysis and any effect due to variation in moisture content or asphalt content is included in the standard error of the slope and intercept. Column headings are as previously defined except that "d.f.", residual degrees of freedom of the regression, has been added.

Representative plots of logarithm strain rate versus deviator stress are shown in Figures 14 and 15. The results shown in these figures and tabulated in Tables 20 through 23 were obtained by holding T_s, T_c and P

Table 20. Deviator stress-strain rate, Series A

Group	D psi	$\dot{\epsilon} \times 10^4$ %/appl	Moisture content %	Regression analysis $\ln \dot{\epsilon}$ vs D Intercept s_e	$\beta/2 \times 10^2$ s_e	d.f.	r
5A	63.7	7.6	7.35	-10.625	5.715	3	0.987
	75.6	23.0	7.77				
	99.5	68.0	7.44	0.529	0.527		
	119.4	300.0	7.73				
	127.4	270.0	7.21				
10A	87.6	2.0	7.29	-15.081	7.611	8	0.993
	95.5	3.5	6.93				
	103.5	7.4	8.69	0.422	0.327		
	111.4	14.0	7.42				
	119.4	37.0	7.69				
	125.4	45.0	7.08				
	139.3	86.0	8.22				
	147.3	300.0	8.07				
	159.2	590.0	6.11				
	167.2	660.0	7.35				
15A	127.4	2.5	6.93	-14.472	5.200	4	0.977
	127.4	-	7.10				
	147.3	14.0	7.31	0.979	0.578		
	159.2	33.0	7.17				
	183.1	78.0	8.08				
	191.0	82.0	6.97				
	207.0	220.0	7.08				
20A	151.2	3.0	8.07	-17.103	5.815	3	0.971
	191.0	15.5	6.92				
	207.0	88.0	7.35	1.681	0.829		
	222.9	98.0	7.28				
	230.8	400.0	7.17				

Table 21. Deviator stress-strain rate, Series B1

Group	D psi	$\dot{\epsilon}$x10^4 %/appl	Moisture content %	Regression analysis ln $\dot{\epsilon}$ vs D			
				Intercept s_e	$\beta/2x10^2$ s_e	d.f.	r
25B1	127.4	1.8	6.71	-17.487	7.294	3	0.972
	143.3	14.0	7.23				
	163.2	32.0	7.88	1.714	1.014		
	191.0	600.0	7.47				
	207.0	500.0	7.18				
40B1	111.4	2.5	6.98	-13.885	5.490	4	0.984
	127.4	18.0	7.00				
	143.3	27.0	6.84	0.803	0.491		
	179.1	150.0	6.80				
	191.0	400.0	7.42				
	207.0	680.0	7.06				
60B1	127.4	10.0	7.58	-14.171	5.787	3	0.998
	127.4	12.0	7.00				
	143.3	26.0	7.49	0.320	0.204		
	163.2	105.0	7.00				
	207.0	1050.0	7.22				

Table 22. Deviator stress-strain rate, Series B2

Group	D psi	$\dot{\epsilon}$ x 10^4 %/appl	Moisture content %	Regression analysis ln $\dot{\epsilon}$ vs D			
				Intercept s_e	$\beta/2x10^2$ s_e	d.f.	r
25B2	183.1	10.0	7.19	-15.343	4.650	2	0.976
	199.0	18.0	7.04				
	199.0	32.0	7.48	1.497	0.727		
	238.8	140.0	8.20				
40B2	199.0	11.0	7.34	-9.678	1.440	0	-
	238.8	62.0	7.61	-	-		
60B2	183.1	10.0	8.06	-12.710	3.131	1	0.995
	199.0	14.0	6.83				
	238.8	55.0	7.69	0.614	0.295		

Table 23. Deviator stress-strain rate, Series C

Group	D psi	$\dot{\epsilon}x10^4$ %/appl	Asphalt content %	Regression analysis ln $\dot{\epsilon}$ vs D Intercept s_e	$\beta/2x10^2$ s_e	d.f.	r
25C	115.4	0.75	3.98	-16.474	6.155	2	0.985
	135.3	2.4	3.98				
	151.2	13.0	3.49	1.151	0.763		
	191.0	74.0	3.49				
40C	99.5	2.0	3.91	-18.555	11.171	2	0.838
	111.4	82.0	3.94				
	119.4	88.0	4.03	6.020	5.138		
	135.3	160.0	4.03				
60C	79.6	12.0	3.94	-19.018	15.397	2	0.998
	91.5	63.0	3.91				
	99.5	290.0	4.04	0.641	0.633		
	111.4	1500.0	4.05				

constant, so the combined effects of these factors are included in the calculated intercept.

Effects of other variable quantities

Effects of all linear terms in equations 41 and 42 can be evaluated by multiple linear regression techniques. The multiple linear regression model assumes that the effect of one variable quantity is unchanged by the level of any other variable quantity. If this assumption is valid for the data obtained in this investigation, the values of β determined within each test group would be the same regardless of the level of any other variable. Since the computed value of β is different for each test group, a statistical test is necessary (Snedecor and Cochran, 1967, pp. 432 ff) to determine if the values of calculated β are significantly different or

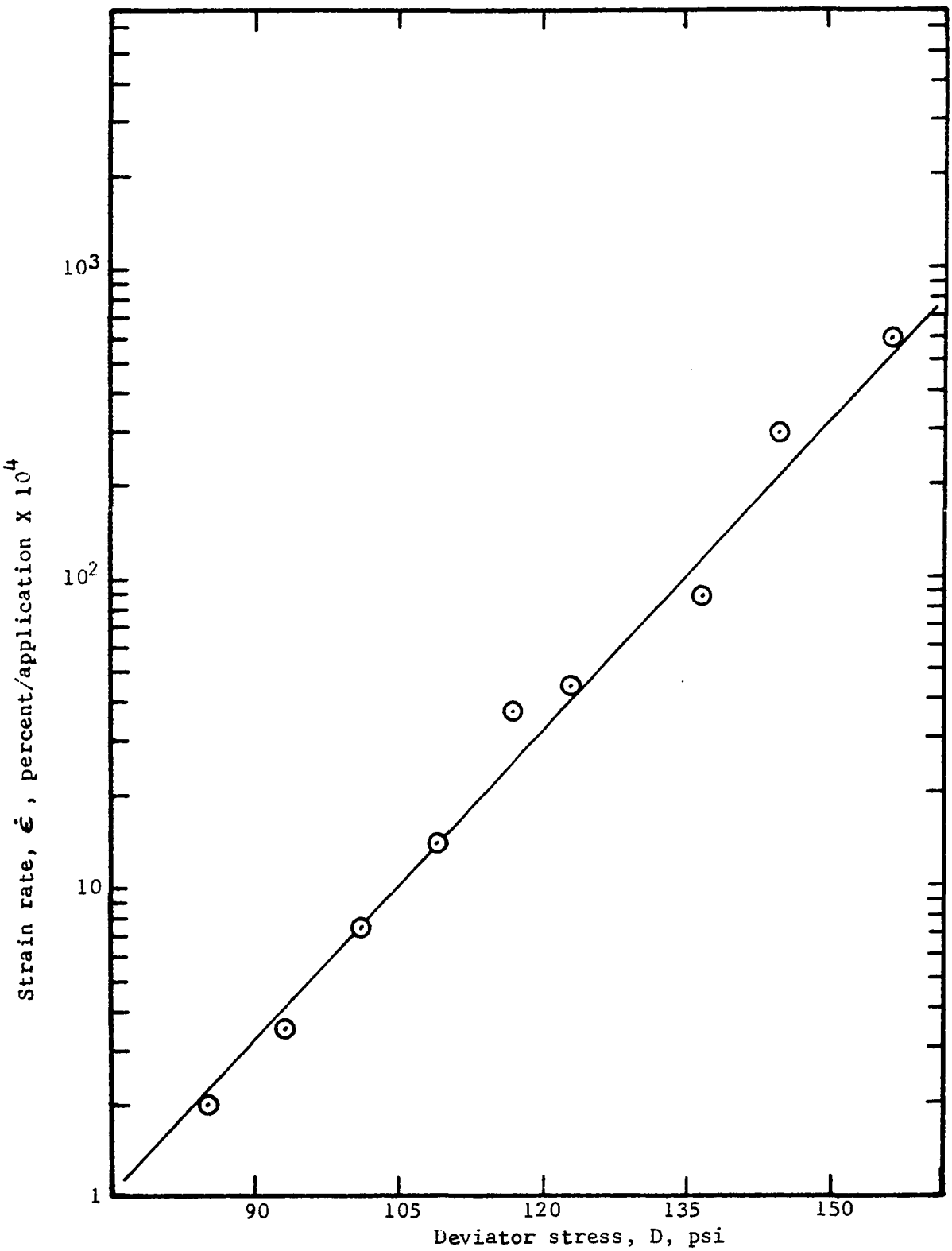

Figure 14. Strain rate variation with deviator stress, Group 10A

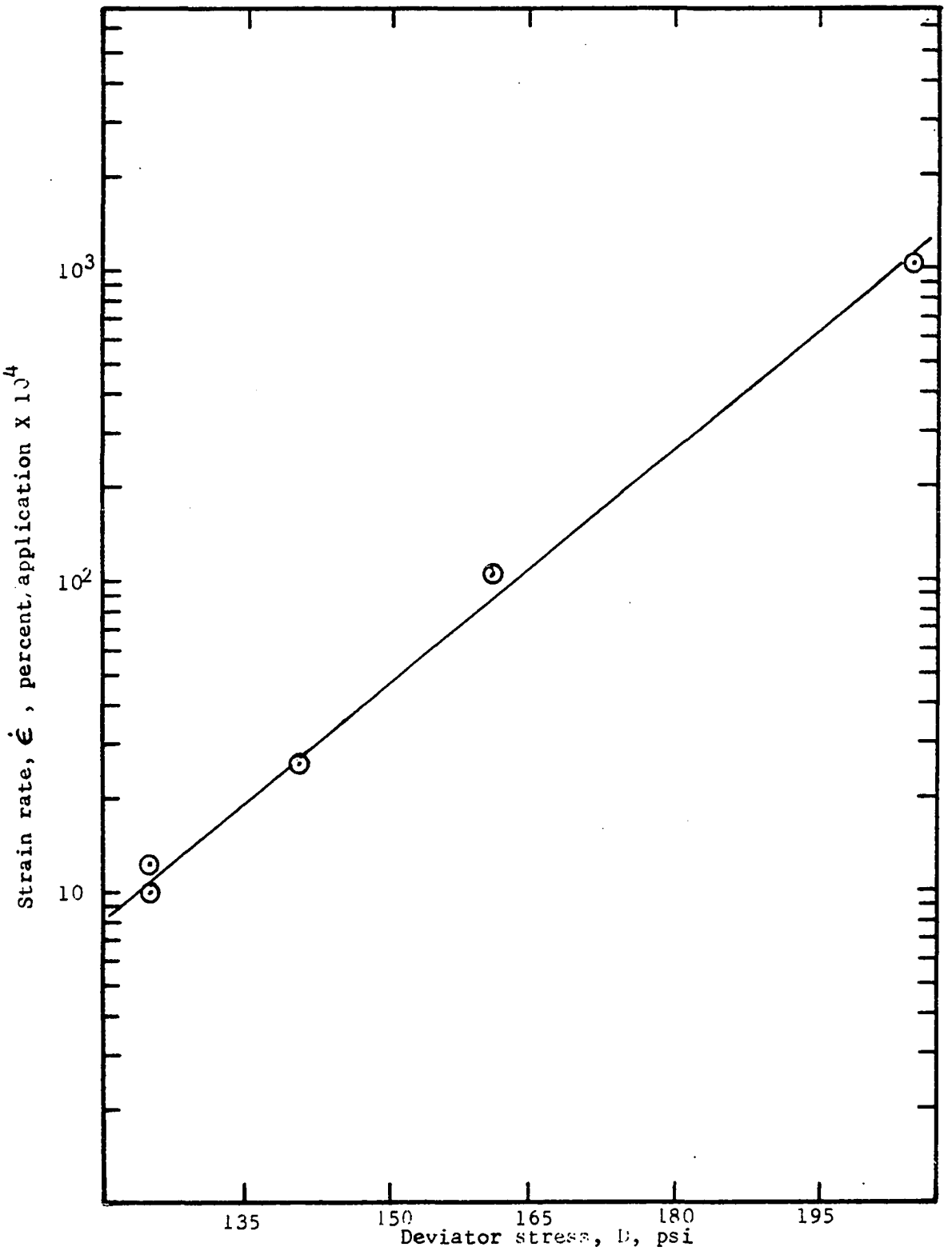

Figure 15. Strain rate variation with deviator stress, Group 60B1

if the differences can be attributed to experimental errors.

Table 24 shows the calculated test statistic for β values calculated from equation 41, the tabulated value of the distribution function for the appropriate degrees of freedom at the 0.01 significance level, and the resulting conclusion for each combination of Groups and/or Series. The conclusions are based on the relative magnitude of the calculated and tabulated values. If the calculated value of the test statistic is less than the tabulated value, the conclusion indicated is that the values of β calculated at different levels of other variables do not significantly differ from one another. Conversely, if the calculated value of the test statistic is greater than the tabulated value, the indicated conclusion is that one or more of the β's are significantly different than some other β values, i.e. not all β's are from the same population.

Table 24. Test for combination of groups and series

Group/series combination	Calculated F	Tabulated $F_{0.01}$	Conclusion
All Groups, Series A	4.99	5.01	May be combined
All Groups, Series B1	2.26	7.56	May be combined
All Groups, Series B2	1.61	30.82	May be combined
Series A and B1	3.07	3.53	May be combined
Series A and B2	5.59	3.81	Cannot be combined
Series A, B1 and B2	3.70	3.06	Cannot be combined
Series B1 and B2	2.92	4.86	May be combined
All Groups, Series C	3.09	10.92	May be combined

As shown in Table 24, if the statistical test indicates that all are from the same population (the variations being attributed to experimental error), the assumption that the effect due to the deviator stress is the same regardless of the level of other variables is valid and those combinations of Groups and/or Series may be combined in a multiple linear regression analysis.

If the statistical test indicates that values are not from the same population, those combinations cannot be analyzed by multiple linear regression techniques. Significant differences in values may be caused by variable effects of deviator stress at different levels of other variables, or such differences may be caused by another variation in the material system that has not been considered in the analysis.

Conclusions based on test statistics calculated for β values determined from equation 42 are the same as those in Table 24. No attempt has been made to combine the results of Series C with the results obtained from any other series, since the asphalt stabilization of Series C made a different material system than that of the other series in the investigation.

Multiple regression analysis

The results of multiple linear regression analyses for those combinations of groups and/or series of tests that may be combined are shown in Tables 25, 26 and 27. In Table 25, strain rate has been considered as the dependent variable and all other quantities, viz. D, p, T_s and T_c as independent variables. In Tables 26 and 27, the number of stress applications at which 2 or 5 percent strain was reached is the dependent variable while independent variables are the same as in Table 25.

Table 25. Multiple regression analysis, Equation 41

Series	p psi	T_c °C	T_s °C	Residual d.f.	Intercept s_e	$\frac{\Delta H^*}{k} \times 10^3$ s_e	$\beta/2 \times 10^2$ s_e	$\frac{\mu}{s_e}$	$\frac{a}{s_e}$	R^2
A	5	25	25	23	-8.775	-	6.233	0.470	-	0.928
	10									
	15				0.326		0.362	0.032		
	20									
			25							
B1	10	60	40	13	-7.482	2.337	6.056	-	-	0.947
			60							
					2.859	0.906	0.396			
			25							
B2	20	60	40	6	-18.422	-1.426	3.772	-	-	0.901
			60		2.679	0.748	0.521			
A and B1	5									
	10	25	25	37	0.748	2.367	6.141	0.464	0.060	0.937
	15	60	40							
	20		60		3.051	0.875	0.263	0.027	0.007	
B1 and B2	10	60	25							
	20		40	21	-8.552	0.637	5.466	0.340	-	0.896
			60		2.642	0.827	0.416	0.032		
								$\frac{\omega}{s_e}$		
			25							
C	10	60	40	9	48.253	19.825	7.618	-		0.794
			60		9.329	3.369	1.688			
			25							
C	10	60	40	8	31.644	19.781	9.306	3.704		0.848
			60		13.045	3.072	1.839	2.205		

Results in Table 25 were obtained from the regression of the logarithm of strain rate on deviator stress as shown in Tables 20 through 23 and the respective levels of other variables shown in Table 25. Results in Tables 26 and 27 were obtained from regression of the logarithm of N_ϵ versus respective levels of deviator stress shown in Tables 16 through 19 and other variables as shown in Tables 26 and 27.

Table 26. Multiple regression analysis, Equation 42, 2 percent strain

Series	p psi	T_c °C	T_s °C	Residual d.f.	Intercept	$\frac{\Delta H^*}{k}\times 10^3$	$\beta/2\times 10^2$	μ	a	R^2
						s_e	s_e	s_e	s_e	
A	5	25	25	24	7.308	-	5.005	0.261	-	0.802
	10				0.493		0.534	0.047		
	15									
	20									
			25							
B1	10	60	40	13	4.194	1.490	3.678	-	-	0.917
			60		2.222	0.704	0.307			
			25							
B2	20	60	40	6	5.802	-0.190	0.756	-	-	0.852
			60		0.666	0.186	0.129			
A and B1	5	25								
	10	60	25	38	0.181	1.753	4.410	0.219	0.036	0.816
	15		40		0.419	1.202	0.354	0.036	0.009	
	20		60							
B1 and B2	10	60	25	21	0.574	1.612	2.574	0.147	-	0.668
	20		40		2.826	0.915	0.419	0.030		
			60					ω		
								s_e		
			25							
C	10	60	40	7	-28.194	11.205	5.047	0.834		0.859
			60		7.089	1.697	0.996	1.185		

Two regression analyses are shown in Table 25 for the combinations of all groups in Series C, one in which the variables are as indicated above and the other (last line in Table 25) in which asphalt content of the specimen was included as an independent variable, assuming a linear relationship between logarithm of strain rate and asphalt content. The coefficient of asphalt content is designated as ω. As can be seen from comparison of these two analyses for Series C, the inclusion of asphalt content did improve regression results; i.e. the value of R^2 increased when asphalt

Table 27. Multiple regression analysis, Equation 42, 5 percent strain

Series	P psi	T_c °C	T_s °C	Residual d.f.	Intercept s_e	$\frac{\Delta H^*}{k} \times 10^3$ s_e	$\beta/2 \times 10^2$ s_e	μ s_e	α s_e	R^2
A	5	25	25	24	8.125	-	6.069	0.455	-	0.688
	10				0.773		0.837	0.074		
	15									
	20									
			25							
B1	10	60	40	13	10.269	1.180	5.302	-	-	0.885
			60		3.830	1.214	0.530			
			25							
B2	20	60	40	6	19.453	-1.795	3.719	-	-	0.842
			60		3.323	0.925	0.692			
A and	5									
B1	10	25	25	38	1.522	1.332	5.725	0.430	0.077	0.755
	20		60		6.390	1.832	0.539	0.055	0.014	
B1 and										
B2	10	60	25							
	20		40	21	11.116	-0.132	4.922	0.272	-	0.854
			60		2.862	0.895	0.457	0.033		
								$\frac{\omega}{s_e}$		
			25							
C	10	60	40	8	-26.125	11.624	6.072	0.610		0.773
			60		10.886	2.797	1.419	1.157		

content was included. Regression analyses of results from Series C reported in Tables 26 and 27 include asphalt content as an independent variable. Multiple regression analyses of the other combinations of groups and series were also made in which moisture content of each specimen was included as an independent variable. However, the largest change in the value of R^2 was 0.003 regardless of the inclusion of moisture content as a variable.

The minor change in regression results due to the moisture content variable may be attributable to a number of factors, one of which is that

for the granular materials investigated, the effect of moisture content may be relatively small. With the narrow range of moisture content used, any such effect has been masked by other experimental variations. Another probable cause is that the moisture content used in the regression analysis was the moisture content determined for each specimen during the molding process, which is not necessarily the moisture content of the specimen when it was sheared. Unlike the asphalt content of specimens in Series C, moisture content of specimens in Series A, B1, and B2 was changed after molding by consolidation and especially by the cooling process as previously discussed.

It is probable that both factors discussed above are partial causes for the result that moisture content has no apparent effect on strain rate. Determination of the effect of moisture content on the rate of deformation would require that a larger range of moisture content be used in the investigation and that moisture content of the specimen at the time it is sheared be determined and used as the value of moisture content in regression analysis.

Again it should be noted that values of the intercept as shown in Tables 25, 26 and 27 are calculated values obtained by extrapolating equation 41 or 42 to zero values of all independent variables. In many cases, no physical significance can be attached to the value of the intercept. This is especially true in those regression analyses in which shear temperature, T_s is included as a variable since it appears in the equations as the reciprocal of absolute temperature, the intercept is obtained by extrapolating

the reciprocal of absolute temperature, as well as the other independent variables, to zero. As can be seen from Tables 25, 26 and 27, the value of the intercept calculated in this manner is greatly dependent on the value of $\frac{\Delta H^*}{k}$.

Figure 16 shows the effect of deviator stress on strain rate for different levels of confining pressure for all groups in Series A. The lines have been obtained from the calculated regression coefficients in Table 25 and the plotted points are observed data.

Figures 17 and 18 are plots of the logarithm of strain rate versus reciprocal of absolute temperature for different levels of deviator stress for Series B1 and C respectively. As before, the lines have been calculated from the regression coefficients in Table 25 and the points are observed data.

Volume change relationships Equation 41 was derived by combining the effects of consolidation pressure and normal stress, setting their coefficients ($\beta \frac{\Delta V}{V}$ and γ) equal to an experimentally determined coefficient, μ. The results of multiple linear regression analyses indicate that equation 41 is an adequate representation of material behavior and that replacement of $\beta \frac{\Delta V}{V} + \gamma$ by μ is a reasonable approximation.

In the development of the failure criterion $\ddot{\epsilon} = 0$ it was shown that $\dot{\ddot{\epsilon}} = \dot{\epsilon}\left[-\beta P_n \frac{d\,\Delta V/V}{dN} - \frac{2}{\epsilon}\frac{d\epsilon}{dN}\right]$ (equation 25b). This implies that when $\ddot{\epsilon}$ is greater than zero (strain acceleration positive), $-\beta P_n \frac{d\,\Delta V/V}{dN}$ must be greater than $\frac{2}{\epsilon}\dot{\epsilon}$.

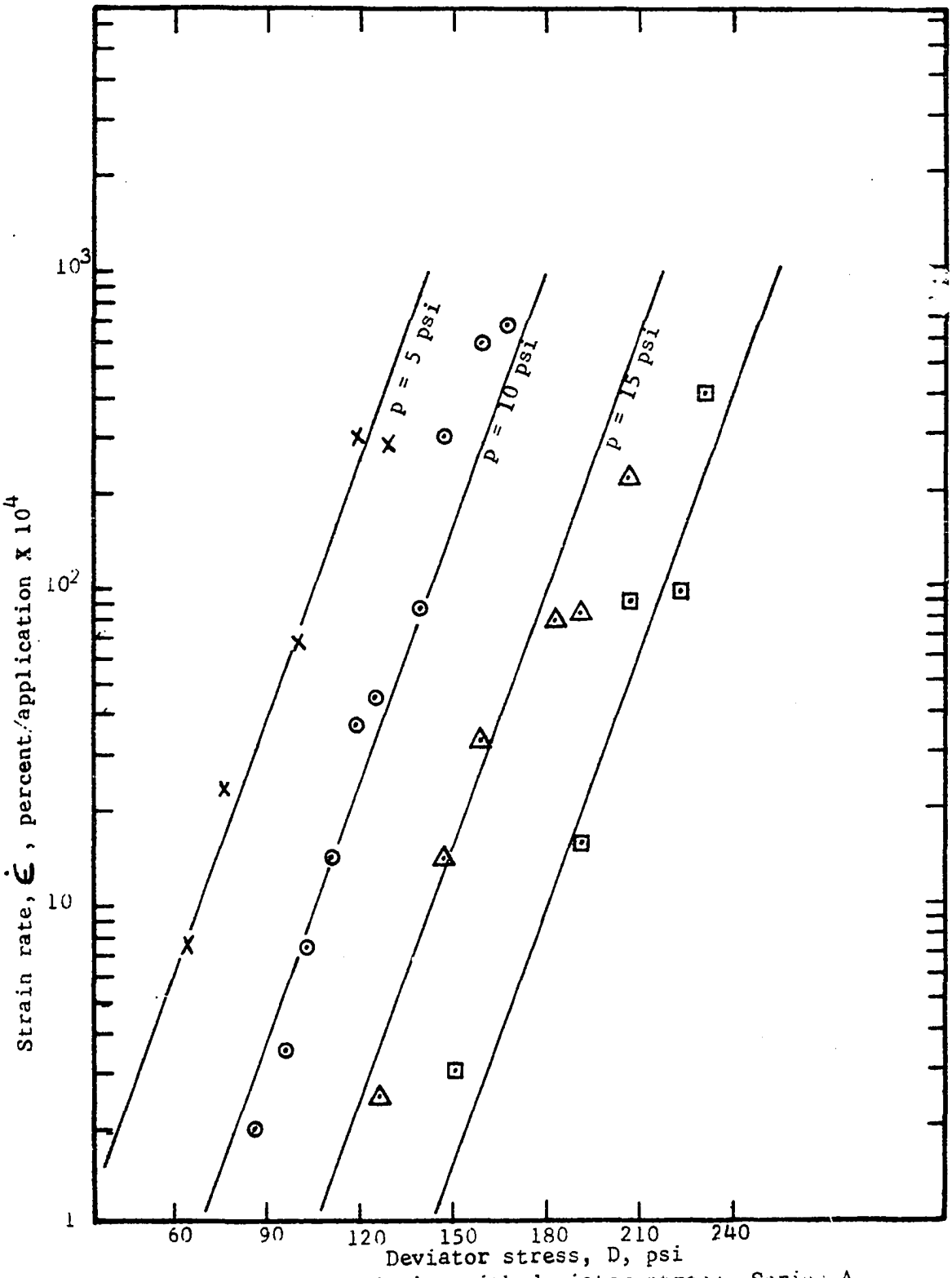

Figure 16. Strain rate variation with deviator stress, Series A

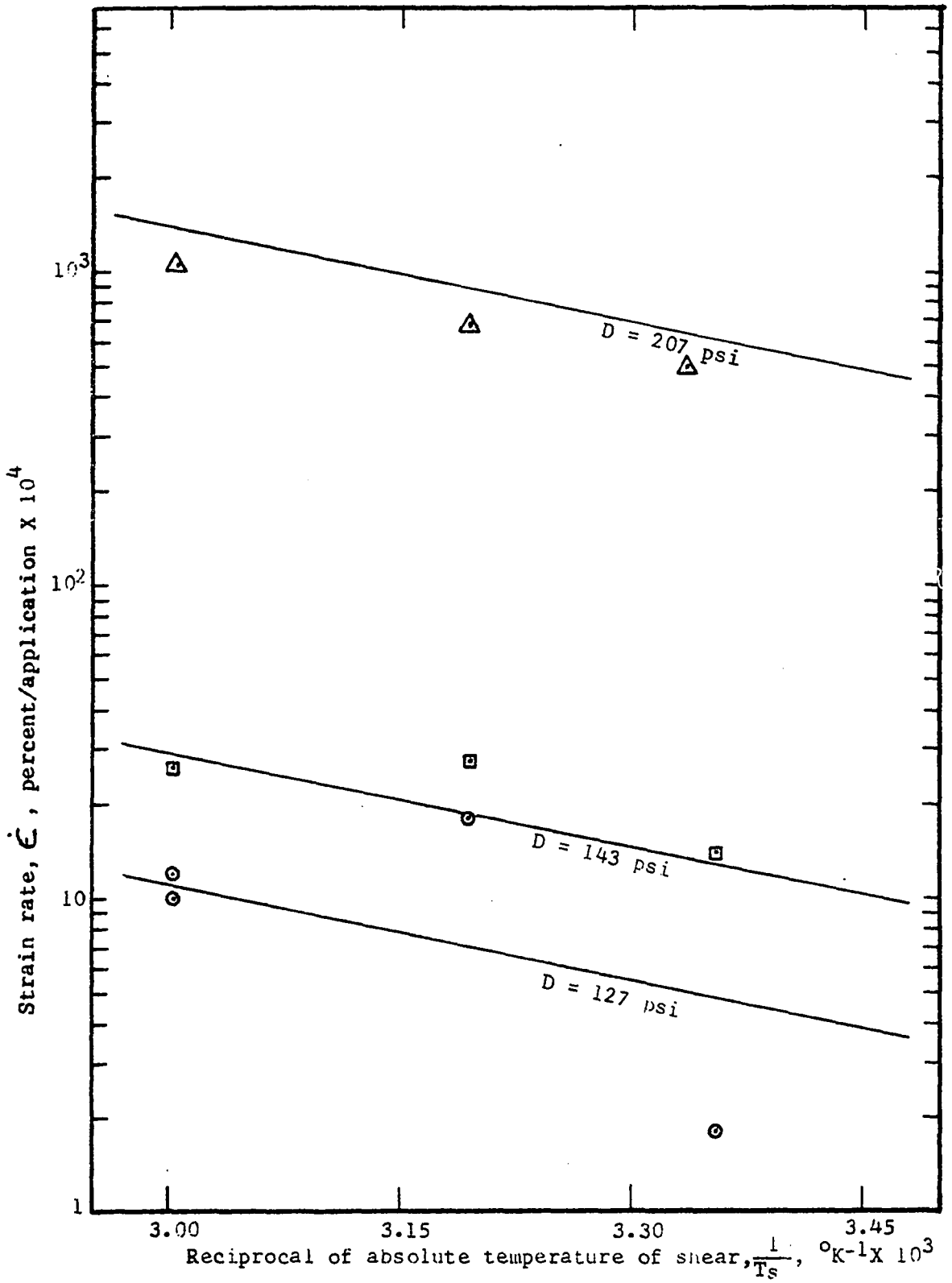

Figure 17. Strain rate variation with shear temperature, Series Bi

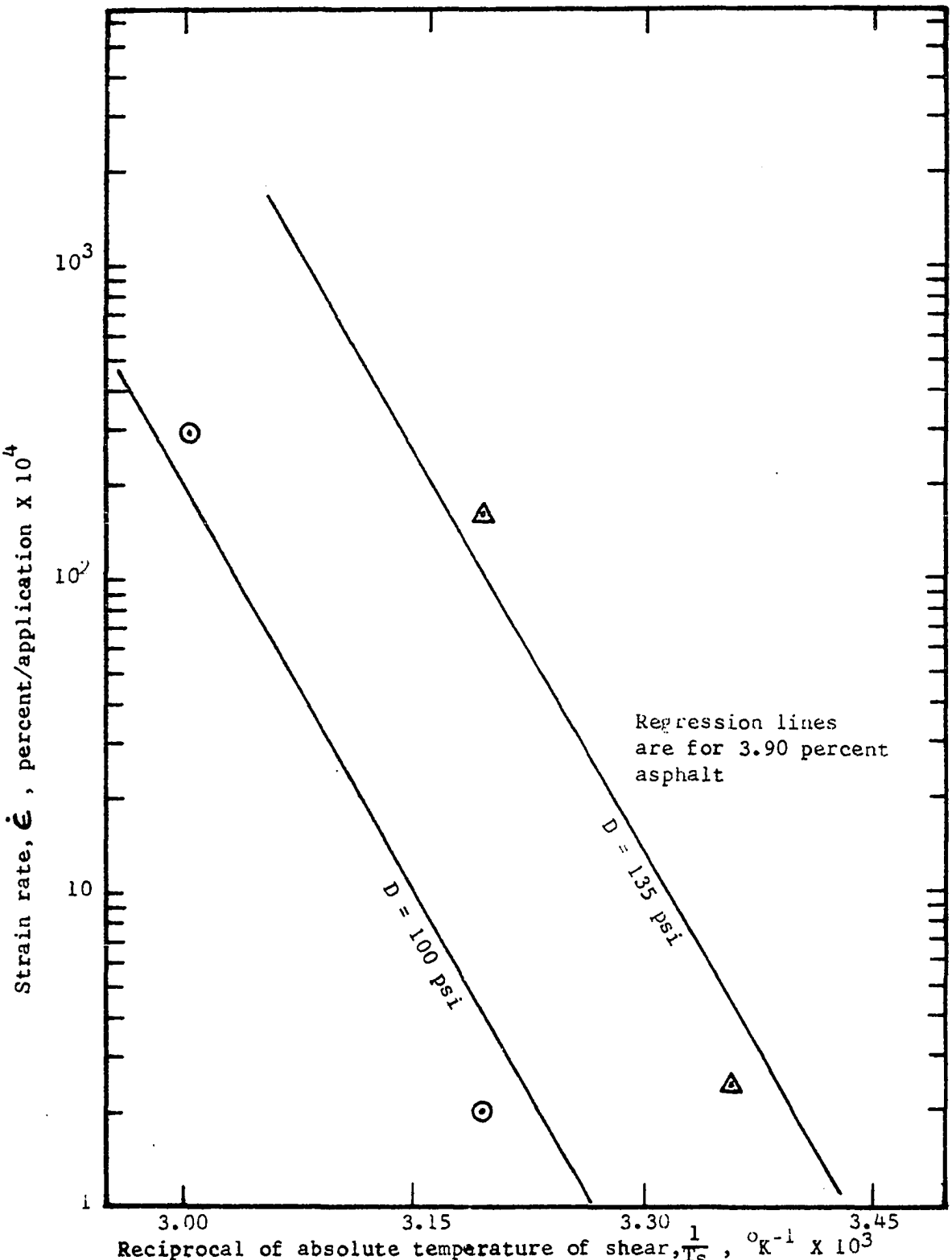

Figure 18. Strain rate variation with shear temperature, Series C

Figure 19 shows strain and volume change data versus number of deviator stress applications for a test in Group 40B2, D = 199.0 psi. The relationships of strain rate and rate of volume change are graphically indicated in this figure. The values of $\beta P_n \frac{d\,\Delta V/V}{dN}$ and $\frac{2}{\epsilon}\dot{\epsilon}$ at different points on the curve (calculations of which are shown in the Appendix) also demonstrate the relationship of rate of volume change and rate of deformation. At 6,000 applications of deviator stress, the values of $\beta P_n \frac{d\,\Delta V/V}{dN}$ and $\frac{2}{\epsilon}\dot{\epsilon}$ are 1.4×10^{-3} and 24.2×10^{-3} respectively, indicating that at this point, $\dot{\epsilon}$ is decreasing. At 6800 applications the values are 25.7×10^{-3} and 24.6×10^{-3} respectively, indicating an increasing rate of deformation.

The data from this particular test specimen demonstrates the implications of the relationship expressed by equation 25b, i.e. as the rate of volume change becomes negative, the rate of strain increases sharply. Not all of the other test data exhibit the relationship of increasing strain rate and decreasing rate of volume change to such a marked degree as is shown in Figure 19. Further confirmation of the relationships between rate of strain and rate of volume change will require greater precision and sensitivity of volume change and deformation measurements than were used in this investigation.

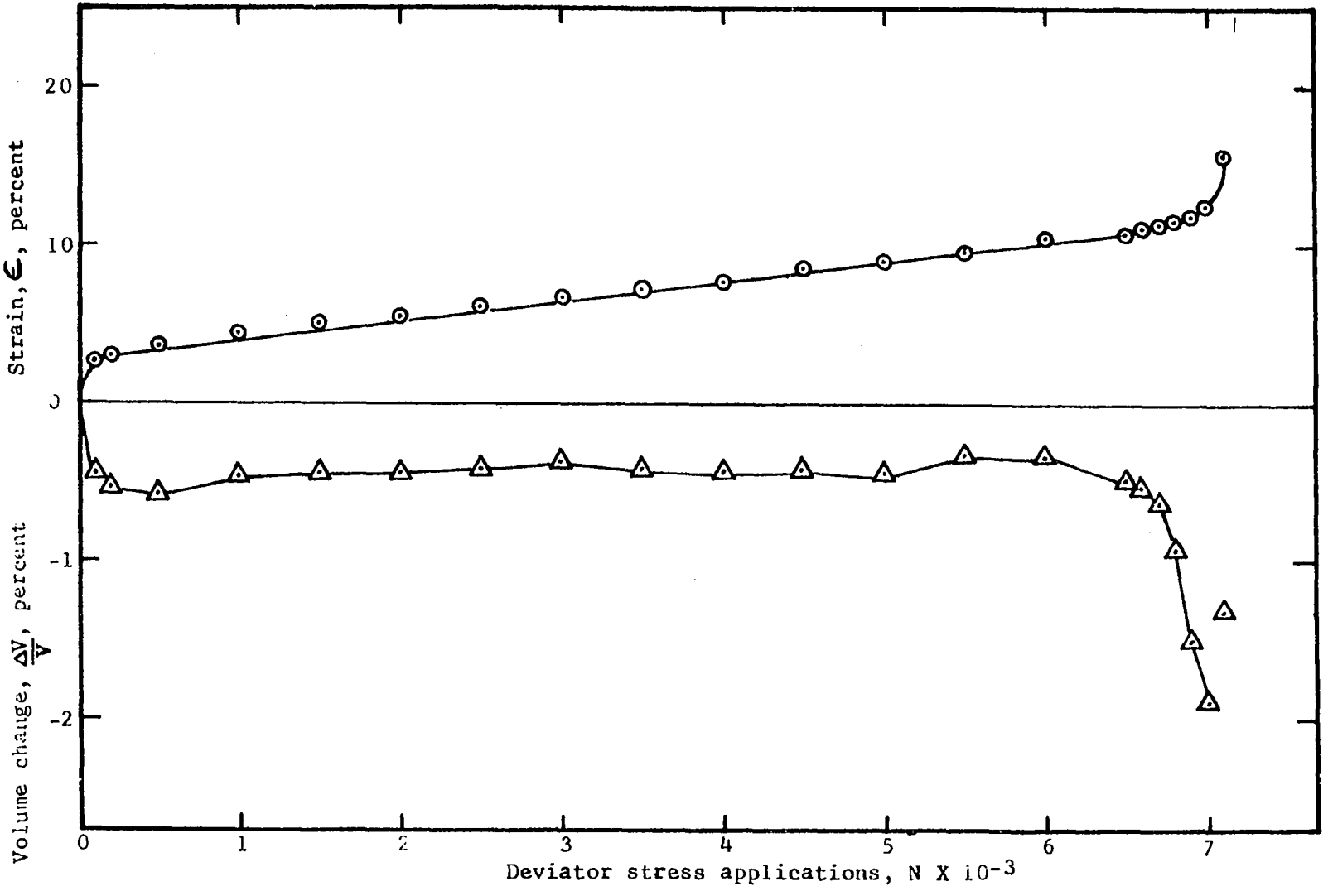

Figure 19. Axial strain and volume change versus deviator stress applications, Group 40B2, 199 psi

DISCUSSION AND CONCLUSIONS

Discussion

Results of this investigation show that the initial transient creep portion of the number of applications versus deformation curve is described by equation 18. The total strain that can be represented by this equation varies from 2.74 to 8.97 percent for untreated specimens and from 0.88 to 5.63 percent for the asphalt treated specimens.

In the tests on untreated material, there is no apparent trend that indicates that the total strain over which equation 18 describes material behavior is related to deviator stress, confining pressure, consolidation temperature or shear temperature. In the asphalt treated specimens of Series C, the total strain described by equation 18 is apparently related to shear temperature as seen in Table 13, while there is no apparent trend with deviator stress. Consolidation pressure and temperature and confining pressure were constant in Series C.

As noted in development of the model equations used in analysis of results in this investigation, equation 18 is entirely empirical. No generally accepted interpretation of the theoretical significance of this relationship is known. It is possible that, at least in particulate systems such as were studied in this investigation, the number of bonds at the interparticle contacts increase in proportion to the reciprocal of deformation squared. While such a hypothesis is purely conjectural, such a mechanism would not be contrary to the energy barrier concept of resistance to deformation.

The relationship between shear temperature and range of strain over which equation 18 is applicable, as observed in Series C, may also occur in untreated materials, but the higher activation enthalpy of asphalt treated material makes the effect more apparent.

In developing the model equations, β was assumed to be a constant equal to $\frac{\beta'}{k\ T_s}$. If β is a constant, β' must vary inversely as T_s. As has been shown in Table 24, the experimental values of β cannot be assumed to be equal for all of the untreated material. However, in those combinations of test groups or series where T_s was the only variable, i.e. combination of groups in Series B1, B2 and C, it has been shown that β can be considered constant. This implies that the variation in the value of β is due to some reason other than changes in shear temperature.

Three values of β have been calculated for each test group, one each from equation 42 at 2 and 5 percent strain (Tables 16 through 19) and one from equation 41 (Tables 20 through 23). Values of β for each test group generally agree quite well, the most notable exceptions being Series B2 and Group 40C. Since development of equation 42 involved an approximation that the effect of ϵ_o be negligible, it might be anticipated that those determinations of β from equation 42 would be subject to greater error than those calculated from equation 41. The correlation coefficient of a regression analysis is a measure of how well the observed data fits the model equation. Therefore, correlation coefficients should indicate if one model equation describes observed data better than another.

Considering only deviator stress as an independent variable, the mean

correlation coefficients from equation 42 at 2 and 5 percent strain are 0.934 and 0.957 respectively. Considering the same independent variable, the mean correlation coefficient from equation 41 is 0.973. A test to determine if these differences are statistically significant indicates they are not. Based on results of this investigation, equation 41 does not provide a significantly better estimate of the value of β than does equation 42 at constant levels of p, T_c and T_s.

When p, T_c and T_s are included as variables, mean values of the multiple R^2 for equation 42 at 2 and 5 percent strain are 0.819 and 0.800 respectively; for equation 41 the mean R^2 is 0.910. These differences are found to be statistically significant when either of the values from equation 42 are compared to that from equation 41. The difference between R^2 values calculated from equation 42 is not significant.

When all variables are considered, equation 41 describes observed behavior better than equation 42 and values of material parameters calculated from equation 41 are subject to less error than those from equation 42. This is probably due to the fact that equation 42 does not adequately describe the effect of structure when p, T_c and T_s are varied. Since equation 41 provides the best estimates of material parameters, those values shown in Table 25 have been used in making comparisons with the results reported by other investigators.

The value of α has been determined using only two levels of consolidation temperature, thus leaving it poorly defined.

Values of μ determined with four levels of confining pressure in Series A and combination of Series A and B1 is consistent. In the combination of

Series B1 and B2, the value is somewhat less than other determinations, but Series B1 and B2 have only two levels of confining pressure. Because this coefficient contains the effects of both consolidation pressure and normal stress, it is difficult to compare this value with the results of other investigators who used direct shear tests. The value of μ is on the order of 10 times the value of the coefficient for normal stress determined by Noble (1968) from direct shear tests on silt. Part of this difference is a result of the combination of effects of P_n and P_c in this investigation, but much of the difference is probably a result of the greater volume change necessary for deformation of the granular materials used in this investigation.

Values of β are quite consistent for all combinations of groups or series with the notable exception of Series B2. Also, the value of $\frac{\Delta H^*}{k}$ for Series B2 is of opposite sign than other determinations. A negative value of $\frac{\Delta H^*}{k}$ would mean that a decrease in shear temperature would cause an increase in the rate of deformation. This is not possible unless the decrease in shear temperature also induces other changes in the material. As has been discussed previously, as the temperature of the specimen was lowered, the moisture content increased. During the experimental phase of the investigation, based on preliminary results from Series B1, it was thought that any changes in moisture content during cooling would have a negligible effect on the rate of deformation. It must be concluded, however, that in Series B2 this effect is not negligible.

The correlation coefficients in Tables 21 and 22 indicated less variation in those test groups in which the shear temperature was equal to the

consolidation temperature than in those in which the shear temperature was less than consolidation temperature. Results of the statistical tests shown in Table 24 indicate that results of Series B2 cannot be combined with any other series except B1. Thus, when Series B1 and B2 are considered, the differences are not significant, but when Series B2 is considered in any other combination, results of Series B2 are significantly different than results of other series.

From comparison of results obtained from various combinations of test groups and series, it appears that the results from Series B2 are unreliable and that this is attributable to changes in moisture content during cooling. Since the results of Series B1 are apparently not affected greatly, it is probable that the amount of change in moisture content due to cooling is related to confining pressure. Because of the apparent unreliability of results from Series B2, they have not been used in making comparisons with results reported by others.

Values of β', the volume of a flow unit, for treated and untreated material are shown in Table 28 with the results of other investigators for comparison. Calculations of β' from β are shown in the Appendix.

Experimentally determined values of β' are probably average flow unit volumes. Table 28 indicates that the average flow unit volume in untreated material decreases as clay content decreases. Consideration of the types of bonds in particulate systems, i.e. bonds between water layers on clay mineral surfaces and at points of contact between larger solid particles, provides a basis for interpretation of the relationship between clay content and average flow unit volume.

Table 28. Volume of a flow unit at 300 ^{o}K

Material	Reference	Clay content <2 micron %	$\beta' \times 10^{-4}$ A^3	$\sqrt[3]{\beta'}$ A
Clay	Noble, 1968	80.4	67.1	87.6
Silt	Noble, 1968	26.0	14.2	52.1
Granular material	This study	1.7	7.4	42.0
Asphalt cement	Moavenzadeh and Stander, 1966	-	37.0	71.9
Asphalt cement	Herrin and Jones, 1963	-	39.9	73.5
Asphalt treated granular material	This study	1.7	11.2	48.2

When the percentage of clay is high, the flow unit approaches the size of clay mineral platelets approximately 10 Angstroms thick. As the clay content decreases, bonds associated with clay mineral surfaces have less effect on the average size of an experimentally determined flow unit and flow unit size approaches that of distances between asperities on solid particle surfaces. As shown in Table 28, the flow unit size for material with very low clay content is still considerably larger than inter-atomic dimensions.

Experimental values of β' for asphalt treated material are roughly one-third of the values reported by Moavenzadeh and Stander (1966) and Herrin and Jones (1963) for 60 to 70 penetration grade asphalt cements. The flow unit size of asphalt treated material is probably dependent on the asphalt film thickness on the granular particles. If so, flow unit volume should vary with asphalt content, approaching that of asphalt cement at higher asphalt contents. The coefficient of asphalt content, ω, would then represent the change in β' due to change in film thickness, or asphalt content. Where asphalt content was included as a variable, it was found that

the rate of deformation increased with increased asphalt content, which would coincide with an increase in β.

Confirmation of this interpretation of the effect of asphalt content on rate of deformation will require investigation of material with greater ranges of asphalt content than were used in this study. Also, any interrelationships between flow unit size, asphalt content and gradation of material would need to be determined.

Activation enthalpy, ΔH^*, can be determined from the coefficient of $\frac{1}{T_s}$ in equation 41. Values of activation enthalpy for the materials in this investigation, with results reported for several other materials for comparison, are shown in Table 29.

The value of ΔH^* for asphalt cement from Herrin and Jones (1963) is the average of five values determined from strain rates and shear temperatures at each of five levels of shear stress. These values of ΔH^* were determined from regression of the logarithm of strain rate on the reciprocal of absolute temperature at constant shear stress; the determinations thus made ranged from 43.4 to 46.8 kcal per mole. The analysis reported by Herrin and Jones assumed a hyperbolic sine relationship between strain rate and shear stress. They determined material parameters at each temperature by choosing values of the parameters which best fit their data; values thus determined were used to evaluate ΔH^*. The value of ΔH^*, 62 kcal per mole, reported by Herrin and Jones differs considerably from the value of 44.6 calculated from their data. However, calculation of ΔH^* from strain rate and shear temperature at constant shear stress does not involve intermediate steps or empirically determined material parameters.

Table 29. Activation enthalpy

Material	Reference	ΔH^* kcal/mole
Metals	Finnie and Heller, 1959	50
Concrete	Polivka and Best, 1960	54
Asphalt cement (penetration 72)	Herrin and Jones, 1963	44.6
Asphalt cement (penetration 63)	Moavenzadeh and Stander, 1966	21.0
Asphalt cement (penetration 30)	Moavenzadeh and Stander, 1966	32.0
Asphalt treated granular material	This study	39.4
Snow	Landauer, 1955	14
Ice	Barnes and Tabor, 1966	29.7
Ice	Glen, 1953; 1955	31.4
Ice	Gold, 1967	15
Water	Glasstone et al., 1941	4-5
Soils	Mitchell et al., 1968	25-45
Soil (clay)	Noble, 1968	12-29
Soil (silt)	Noble, 1968	4-7
Granular material	This study	4.7

Values of activation enthalpy of asphalt cement and asphalt treated granular materials are of the same order of magnitude. The activation enthalpy of asphalt treated granular material is probably influenced greatly by the activation enthalpy of the asphalt cement used. Comparison of the activation enthalpy of various asphalt cements in Table 29 indicate that penetration grade and activation enthalpy are not closely related.

The activation enthalpy of untreated granular material determined in this study agrees closely with that reported by Noble (1968) for silt and approximates the activation enthalpy of water. The hydrogen bond energy in water is approximately 5 or 6 kcal per mole (Rodebush and Buswell, 1958; Fyfe, 1964, p. 92). This agreement between hydrogen bond energy and activation enthalpy of untreated material indicates that bonds in untreated material may consist of hydrogen bonds between adsorbed water molecules on the mineral surface.

Suggestions for further research

Based on the results of this investigation, the effects of several of the variable quantities studied need further clarification. Also, extension of these findings to more general material systems will require determination of the effects of several quantities that were not studied herein. The following are suggested as items for further investigation:

1) Behavior of granular materials with a wider range of asphalt and water contents.
2) Separate determination of the effects of consolidation pressure and normal stress.
3) Effects of clay content or other variations in gradation on flow unit size.
4) Relationships of asphalt cement properties and activation enthalpy of asphalt treated materials.
5) An effort to determine the functional relationship of structure to deformation and volume change at various levels of shear and normal stress.

6) Relationships between the range of transient creep and conditions of shear temperature and shear and normal stress.

7) Effect of consolidation temperature on rate of deformation be extended to asphalt treated materials.

8) Effects of frequency and duration of stress application on deformation rate. This is especially important if the findings of this investigation are to be extended for use in pavement design where not only the magnitude of imposed stresses but also the frequency of application (traffic density) and duration of stresses (traffic speed) may be of great importance.

9) Relationships between asphalt content, material gradation and flow unit size.

10) Effects of combinations of pore fluids, e.g. water and asphalt cement, in varying proportions, on activation enthalpy and flow unit size.

Conclusions

A model for the behavior of granular material subjected to repeated loads is proposed. This model is based on bonds formed at interparticle contacts, resistance to rearrangement of particles, and internal structure of the material. Stresses applied to the material are transferred through the bonds, and deformation of the material takes place by distortion of breaking of bonds and rearrangement of particles. The total resistance to deformation constitutes an energy barrier to deformation of the material mass, termed the activation energy. This energy barrier may be surmounted by bonds having sufficient thermal and mechanical energy.

Based on this model of resistance to deformation, an equation was developed beginning with the Arrhenius equation of chemical kinetics. Separation of the contributions of various factors to the activation energy enabled determination of their individual effects. Equation 41 was shown to describe the observed behavior of both untreated and asphalt treated granular materials over the range of variables considered.

Using the equation developed from the energy barrier concept and an empirically determined relationship between total strain and number of applications of stress, an integrated equation was developed to relate number of applications of stress with other variables at fixed levels of deformation. Equation 42 was found to describe material behavior over the ranges of deviator stress considered, when other variables were held constant. However, equation 42 did not describe observed material behavior, over the range of all variables considered, as well as did equation 41 based only on energy barrier concepts.

Experimental tests, consisting of 64 repeated load triaxial compression tests on an untreated and asphalt treated granular material provided the following observations:

1) Repeated load triaxial compression tests yield a linear relationship between the logarithm of strain rate and deviator stress. The proportionality coefficient may be used to evaluate the volume of a flow unit. This volume was found to be considerably smaller than that reported by others for finer grained materials.

2) Activation enthalpies obtained from coefficients of the relationship between logarithm of strain rate and reciprocal of absolute temperature

of shear were found to be approximately the same as the activation enthalpy of the pore fluid.

3) Repeated load tests yield a linear relationship between the logarithm of stress applications at constant strain and deviator stress. The proportionality coefficient in the model equation is the same as the coefficient for deviator stress-logarithm of strain rate relationship. Experimentally determined values from each of the two methods are, in most cases, in close agreement.

4) Activation enthalpies determined from equation 41, based on strain rate, differ by approximately 50 percent from those determined from equation 42 based on total strain. Because the multiple linear regression correlation coefficients for equation 41 are higher than those of equation 42, activation enthalpies determined from equation 41 are considered better estimates.

5) Increased temperature of consolidation was found to decrease the rate of deformation, but the relationship is poorly defined since only two levels of consolidation temperature were used.

6) Increased confining pressure in the triaxial cell caused a decrease in the rate of deformation. This effect is interpreted as a decrease in the size of flow units as the confining pressure is increased. Test methods used in this investigation did not permit determination of separate effects of normal stress and consolidation pressure.

This study of behavior of granular materials subjected to repeated loads has yielded equations which reasonably describe deformation behavior of the materials. However, modification of equation 42 will probably be

required if it is to describe material behavior as well as equation 41. Interdependency of some measured quantities, e.g. volume change, pore pressure and confining pressure, may dictate other modifications of the equations as their effects become more completely understood. Further investigation based on the equations proposed herein would seem justified in order to confirm, and extend to a wider range of materials and other variables, the findings of this investigation. The model equation describes material behavior under stress conditions very similar to those imposed on pavement structures in terms of fundamental parameters which might be used as a rational basis for analysis of pavement deformations.

BIBLIOGRAPHY

Abdel-Hady, Mohamed and Moreland Herrin. 1965. Rheological properties of compacted soil-asphalt mixtures. Highway Research Record 91: 13-35.

Andrade, E. N. da C. 1951. Viscosity and plasticity. Chemical Publishing Company, Inc., New York, New York.

Andrade, E. N. da C. 1957. The concept of creep. In Creep and Recovery. Proceedings of seminar on Creep and Recovery of Metals. Pp. 176-198. American Society for Metals, Cleveland, Ohio.

Barnes, P. and D. Tabor. 1966. Plastic flow and pressure melting in deformation of ice. Nature 210: 878-882.

Best, T. W. and J. M. Hoover. 1966. Stability of granular base course mixes compacted to modified density: special report. Engineering Research Institute, Iowa State University of Science and Technology, Ames, Iowa.

Bowden, F. P. and D. Tabor. 1950. The friction and lubrication of solids. Clarendon Press, Oxford, England.

Brown, Stephen F. and Peter S. Pell. 1967. Subgrade stress and deformation under dynamic load. American Society of Civil Engineers Proceedings 93, No. SM1: 17-46.

Campanella, Richard G. and James K. Mitchell. 1968. Influence of Temperature Variations on Soil Behavior. American Society of Civil Engineers Proceedings 94, No. SM3: 709-734.

Caughey, R. H. and W. B. Hoyt. 1954. Effects of cyclic overloads on the creep rates and rupture life of Inconel at 1700 and 1800 F. American Society for Testing and Materials Special Technical Publication 165: 79-102.

Christensen, Richard W. and Tien Hsing Wu. 1964. Analysis of clay deformation as a rate process. American Society of Civil Engineers Proceedings 90, No. SM6: 125-157.

Davis, Edgar F., Edward M. Krokosky and Egons Tons. 1965. Stress relaxation of bituminous concrete in tension. Highway Research Record 67: 38-58.

Dorn, John E. 1957. The spectrum of activation energies for creep. In Creep and Recovery. Proceedings of seminar on Creep and Recovery of Metals. Pp. 255-283. American Society of Metals, Cleveland, Ohio.

Eyring, Henry. 1967. Absolute rate theory of elementary processes, including fast reactions. In Claesson, Stig, ed. Fast reactions and primary processes in chemical kinetics. Pp. 17-31. Interscience Publishers, New York, New York.

Feltner, C. E. and G. M. Sinclair. 1963. Cyclic stress induced creep of close-packed metals. In Joint International Conference on Creep. Pp. 3-9 to 3-15. The Institution of Mechanical Engineers, London, England.

Ferguson, E. G. and J. M. Hoover. ca. 1968. Improvement of granular base course materials with portland cement. Presented at Highway Research Board Meeting, Washington, D.C., January 1968. To be published in Highway Research Record.

Finnie, I. and W. Heller. 1959. Creep of engineering materials. McGraw-Hill Book Company, Inc., New York, New York.

Fyfe, W. S. 1964. Geochemistry of solids. McGraw-Hill Book Company, Inc., New York, New York.

Glasstone, Samuel, Keith J. Laidler and Henry Eyring. 1941. The theory of rate processes. McGraw-Hill Book Company, Inc., New York, New York.

Glen, J. W. 1953. Rate of flow of polycrystalline ice. Nature 172: 721.

Glen, J. W. 1955. The creep of polycrystalline ice. Royal Society of London Proceedings, Series A, 228: 519-538.

Gold, L. W. 1967. Some bulk properties of ice. National Research Council of Canada, Division of Building Research Paper No. 256.

Goughnour, Ray R. and O. B. Andersland. 1968. Mechanical properties of a sand-ice system. American Society of Civil Engineers Proceedings 94, No. SM4: 923-950.

Hahn, Sang Joon, Taikyue Ree and Henry Eyring. 1967. Mechanism for the plastic deformation of Yule Marble. Geological Society of America Bulletin 78: 773-782.

Havers, J. A. and E. J. Yoder. 1957. A study of interactions of selected combinations of subgrade and base course subjected to repeated loading. Highway Research Board Proceedings 36: 443-478.

Haynes, John H. and Eldon J. Yoder. 1963. Effects of repeated loading on gravel and crushed stone base course materials used in the AASHO road test. Highway Research Record 39: 82-96.

Herrin, Moreland and G. Jones. 1963. Behavior of bituminous materials from the viewpoint of absolute rate theory. Association of Asphalt Paving Technologists Proceedings 32: 82-105.

Herrin, Moreland, Charles R. Marek and Richard Strauss. 1966. The applicability of the absolute rate theory in explaining the behavior of bituminous materials. Association of Asphalt Paving Technologists Proceedings 35: 1-17.

Hoover, J. M. 1967. Factors influencing stability of granular base course mixes: final report. Engineering Research Institute, Iowa State University of Science and Technology, Ames, Iowa.

Huang, Y. H. 1967. Deformation and volume change characteristics of a sand-asphalt mixture under constant direct and triaxial compressive stresses. Highway Research Record 178: 60-74.

Hughes, C. S. ca. 1967. Evaluation of a repeated load device through tests on specimens compacted by three different methods. Original not available; abstracted in Highway Research Information Service Abstracts. October 1967.

Kingery, W. D. 1960. Regelation, surface diffusion and ice sintering. Journal of Applied Physics 31: 833-838.

Konder, R. L. and R. J. Krizek. 1960. A non-dimensional approach to the static and vibratory loading of footings. Highway Research Board Bulletin 277: 37-60.

Landauer, Joseph K. 1955. Stress-strain relations in snow under uniaxial compression. Journal of Applied Physics 26: 1493-1497.

Larew, H. G. and G. A. Leonards. 1962. A strength criterion for repeated loads. Highway Research Board Proceedings 41: 529-556.

Manson, S. S. and W. F. Brown, Jr. 1959. Survey of the effects of non-steady load and temperature conditions on the creep of metals. American Society for Testing and Materials Special Technical Publication 260: 65-104.

Mitchell, J. K. 1964. Shearing resistance of soils as a rate process. American Society of Civil Engineers Proceedings 90, No. SM1: 29-61.

Mitchell, James K. and Richard Campanella. 1964. Creep studies on saturated clays. American Society for Testing and Materials Special Technical Publication 361: 90-103.

Mitchell, James K., Richard G. Campanella and Atwar Singh. 1968. Soil creep as a rate process. American Society of Civil Engineers Proceedings 94, No. SM1: 231-253.

Moavenzadeh, F. and R. A. Carnaghi. 1966. Viscoelastic response of sand-asphalt beams on elastic foundations under repeated loading. Association of Asphalt Paving Technologists Proceedings 35: 514-528.

Moavenzadeh, F. and R. R. Stander, Jr. 1966. On flow of asphalt. Highway Research Record 134: 8-35.

Monismith, Carl L. and R. L. Alaxander. 1966. Rheologic behavior of asphalt concrete. Association of Asphalt Paving Technologists Proceedings 35: 400-446.

Moore, Walter J. 1962. Physical chemistry. 3rd ed. Prentice-Hall Inc., Englewood Cliffs, New Jersey.

Noble, Calvin Athelward. 1968. Effect of temperature on strength of soils. Unpublished Ph.D. thesis. Library, Iowa State University of Science and Technology, Ames, Iowa.

Paaswell, Robert E. 1967. Temperature effects on clay soil consolidation. American Society of Civil Engineers Proceedings 93, No. SM3: 9-22.

Pagen, Charles A. 1965. Rheological response of bituminous concrete. Highway Research Record 67: 1-26.

Polivka, M. and C. Best. 1960. Investigation of the problems of creep in concrete by Dorn's method. University of California, Berkeley, California.

Ree, Francis, Taikyue Ree and Henry Eyring. 1963. Relaxation theory of creep of metals. American Society of Civil Engineers Transactions 128, Part 1: 1321-1339.

Ree, Taikyue and Henry Eyring. 1955. Theory of non-newtonian flow. I. Solid plastic system. Journal of Applied Physics 26: 793-800.

Rodebush, Worth H. and Arthur M. Buswell. 1958. Properties of water substance. Highway Research Board Special Report 40: 5-16.

Schmidt, Werner E. 1962a. New concepts of shearing strength for saturated clay soils. Part 1. Sols 1: 31-42.

Schmidt, Werner E. 1962b. New concepts of shearing strength for saturated clay soils. Part 2. Sols 2: 19-26.

Schoeck, Gunther. 1957. Theory of creep. In Creep and Recovery. Proceedings of seminar on Creep and Recovery of Metals. Pp. 199-226. American Society for Metals, Cleveland, Ohio.

Secor, K. E. and C. L. Monismith. 1965. Viscoelastic response of asphalt paving slabs under creep loading. Highway Research Record 67: 84-97.

Seed, H. B. and C. K. Chan. 1957. Thixotropic characteristics of compacted clays. American Society of Civil Engineers Proceedings 83, No. SM4: 1427-1 to 1427-35.

Seed, H. B. and C. K. Chan. 1958. Effect of stress history and frequency of stress application on deformation of clay subgrades under repeated loading. Highway Research Board Proceedings 37: 555-575.

Seed, H. B., Clarence K. Chan and Carl L. Monismith. 1955. Effects of repeated loading on the strength and deformation of compacted clay. Highway Research Board Proceedings 34: 541-558.

Seed, H. B. and Robert L. McNeill. 1956. Soil deformations in normal compression and repeated loading tests. Highway Research Board Bulletin 141: 44-53.

Seed, H. B. and R. L. McNeill. 1957. Soil deformations under repeated stress applications. American Society for Testing and Materials Special Technical Publication 232: 177-196.

Seed, H. B., R. L. McNeill and J. de Guenin. 1958. Increased resistance to deformation of clay caused by repeated loading. American Society of Civil Engineers Proceedings 84, No. SM2: 1645-1 to 1645-28.

Simmons, Ward F. and Howard C. Cross. 1954. Constant and cyclic-load creep tests of several materials. American Society for Testing and Materials Special Technical Publication 165: 149-161.

Singh, Atwar and James K. Mitchell. 1968. General stress-strain-time functions for soils. American Society of Civil Engineers Proceedings 94, No. SM1: 21-46.

Smith, G. V. and E. G. Houston. 1954. Experiments on the effects of temperature and load changes on creep rupture of steels. American Society for Testing and Materials Special Technical Publication 165: 67-76.

Snedecor, George W. and William G. Cochran. 1967. Statistical Methods. 6th ed. Iowa State University Press, Ames, Iowa.

Telford, J. W. and J. S. Turner. 1963. The motion of a wire through ice. Philosophical Magazine 8: 527-531.

ACKNOWLEDGMENTS

The research described in this dissertation is part of a study of the factors affecting behavior of granular base course mixes conducted at the Engineering Research Institute, Iowa State University of Science and Technology sponsored by the Iowa Highway Research Board, Iowa State Highway Commission and the Bureau of Public Roads, U.S. Department of Transportation. Partial support for personal expenses was provided by a Ford Foundation Forgivable Loan during the 1967-68 academic year. These sources of essential financial support are gratefully acknowledged.

The encouragement, guidance a support of Dr. R. L. Handy are acknowledged with sincere appreciation. The author owes a real debt of gratitude to Dr. Turgut Demirel and Professor James M. Hoover for their assistance throughout the investigation. Thanks are also due all members of the Soil Research Laboratory Staff for their assistance during the study.

To Margaret Ann, who assumed additional responsibilities of family management with patience, love and understanding, my gratitude and love.

To Jesus Christ, without whose message of patience and love, I would have found this task inordinately burdensome, my thanks for His life and teaching.

APPENDIX

Calculation of $\beta P_n \frac{d\,\Delta V/V}{dN}$ and $\frac{2}{\epsilon}\dot{\epsilon}$

Group 40B2; D = 199.0 psi

$$P_n = D/2 + p = \frac{199.0}{2} + 20.0 = 119.5 \text{ psi}$$

$\beta = 3.772 \times 10^{-2}$ (from Table 25, Series B2)

6,000 applications

$$\frac{d\,\Delta V/V}{dN} = -0.03 \times 10^{-2} \text{ \% per stress application}$$

$$\dot{\epsilon} = 12.6 \times 10^{-4} \text{ \% per stress application}$$

$$\epsilon = 10.4 \text{ \%}$$

$$\beta P_n \frac{d\,\Delta V/V}{dN} = (3.772 \times 10^{-2})\ (119.5)\ (-0.03 \times 10^{-2}) = -1.4 \times 10^{-3}$$

$$\frac{2\dot{\epsilon}}{\epsilon} = \frac{2}{0.104}\ (12.6 \times 10^{-4}) = 24.2 \times 10^{-3}$$

6,800 applications

$$\frac{d\Delta V/V}{dN} = -0.57 \times 10^{-2} \text{ \% per application}$$

$$\dot{\epsilon} = 14.0 \times 10^{-4} \text{ \% per application}$$

$$\epsilon = 11.4 \text{ \%}$$

$$\beta P_n \frac{d\,\Delta V/V}{dN} = (3.772 \times 10^{-2})\ (119.5)\ (-0.57 \times 10^{-2}) = -25.7 \times 10^{-3}$$

$$\frac{2\dot{\epsilon}}{\epsilon} = \frac{2}{0.114}\ (14.0 \times 10^{-4}) = 24.6 \times 10^{-3}$$

Calculation of flow unit volumes

Example calculation for Series A and B1 combined

$\beta/2$ from Table 25 = $6.141 \times 10^{-2} \frac{in^2}{lb}$

$k = 1.380 \times 10^{-16} \frac{dyne\text{-}cm}{^oK}$; $T = 300\ ^oK$

$\beta' = 1.380 \times 10^{-16} \times 300 \times 2 \times 6.141 \times 10^{-2} \times 14.503 \times 10^{-6}$

$= 7.37 \times 10^{-20}\ cm^3$

$= 7.37 \times 10^{4}\ A^4$.